
Learning Adaptive Classifiers Synthesis for Generalized Few-Shot Learning

Han-Jia Ye*
Nanjing University
yehj@lamda.nju.edu.cn

Hexiang Hu*
University of Southern California
hexiangh@usc.edu

De-Chuan Zhan
Nanjing University
zhandc@lamda.nju.edu.cn

Fei Sha†
Google Research
fsha@google.com

Abstract

Object recognition in real-world requires handling long-tailed or even open-ended data. An ideal visual system needs to reliably recognize the populated visual concepts and meanwhile efficiently learn about emerging new categories with a few training instances. Class-balanced many-shot learning and few-shot learning tackle one side of this problem, via either learning strong classifiers for populated categories or learning to learn few-shot classifiers for the tail classes. In this paper, we investigate the problem of *generalized few-shot learning (GFSL)* — a model during the deployment is required to not only learn about “tail” categories with few shots but simultaneously classify the “head” and “tail” categories. We propose the Classifier Synthesis Learning (CASTLE), a learning framework that learns how to synthesize calibrated few-shot classifiers in addition to the multi-class classifiers of “head” classes with a shared neural dictionary, shedding light upon the inductive GFSL. Furthermore, we propose an adaptive version of CASTLE (ACASTLE) that adapts the “head” classifiers conditioned on the incoming “tail” training examples, yielding a framework that allows effective backward knowledge transfer. As a consequence, ACASTLE can handle *generalized few-shot learning* with classes from heterogeneous domains effectively. CASTLE and ACASTLE demonstrate superior performances than existing GFSL algorithms and strong baselines on *MiniImageNet* as well as *TieredImageNet* data sets. More interestingly, it outperforms previous state-of-the-art methods when evaluated on standard few-shot learning.

1 Introduction

Visual recognition for objects in the “long tail” has been an important challenge to address [32, 58]. We often have a very limited amount of data on those objects as they are infrequently observed and/or visual exemplars of them are hard to collect. As such, state-of-the-art methods (*e.g.* deep learning) can not be directly applied due to their notorious demand of a large number of annotated data [18, 23, 46].

Few-shot learning (FSL) [13, 47, 52] is mindful of the limited instances (*i.e.*, shots) per “tail” concept, which attempts to address this challenging problem by distinguishing between the data-rich “head” categories as SEEN classes and data-scarce “tail” categories as UNSEEN classes. While it is difficult

*Equal Contribution.

†On leave from University of Southern California (feisha@usc.edu)

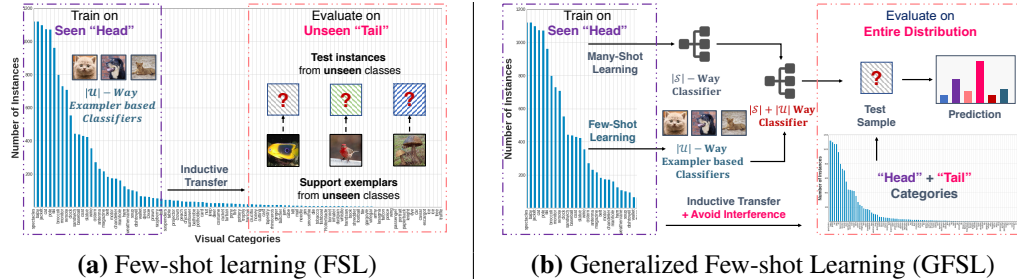


Figure 1: A conceptual diagram comparing the Few-Shot Learning (FSL) and the Generalized Few-Shot Learning (GFSL). GFSL requires to extract inductive bias from SEEN categories to facilitate efficiently learning on few-shot UNSEEN “tail” categories, while maintaining discernability on “head” classes.

to build classifiers with data from UNSEEN classes, FSL mimics the test scenarios by sampling few-shot tasks from SEEN classes data, and extracts inductive biases for effective classifiers acquisition on UNSEEN ones. Instance embedding [44, 47, 52, 60], model initialization [3, 13, 35], image generator [57], and optimization flow [26, 39] act as popular meta-knowledge and usually incorporates with FSL. More details of few-shot learning could be found in an up-to-date survey [25].

This type of learning, however, creates a chasm in object recognition. Classifiers from many-shot learning for SEEN classes and those from few-shot learning for UNSEEN classes do not mix – they cannot be combined directly to recognize *all* object categories simultaneously.

In this paper, we study the problem of *Generalized Few-Shot Learning (GFSL)*, which focuses on the *joint* classification of both data-rich and data-poor categories. Figure 1 illustrates the high-level idea of the GFSL, contrasting the standard FSL. In particular, our goal is for the model trained on the SEEN categories to be capable of incorporating the limited UNSEEN class instances, and make predictions for test instances in both the “head” and “tail” of the entire distribution of categories.

One naive GFSL solution is to train a single classifier over the imbalanced long-tail distribution [17, 32, 58], and rebalance different classifiers [5, 11]. One main advantage of such a joint learning objective over all classes is that it characterizes both SEEN and UNSEEN classes simultaneously. In other words, training of one part (*e.g.*, “head”) naturally takes the other part (*e.g.*, “tail”) into consideration, and promotes the knowledge transfer between classes. However, such a transductive learning paradigm requires collecting the limited “tail” instances in advance, which is violated in many real-world tasks. In contrast to it, our learning setup requires an *inductive* modeling of the “tail”, which is therefore more challenging as we assume no knowledge about the UNSEEN “tail” categories is available during the model learning phase.

There are two main challenges in the inductive GFSL problem, including how to construct the many-shot and few-shot classifiers in the GFSL scenario and how to calibrate their predictions.

First, the “head” and “tail” classifiers for a GFSL model should encode different properties of all classes for high discerning ability, and the classifiers for the many-shot part should be adapted based on the “tail” concepts accordingly. For example, if the UNSEEN classes come from different domains incrementally, a single SEEN classifier is difficult to handle their diverse properties and should not be left alone in this dynamic process. Furthermore, as observed in the generalized zero-shot learning scenario [9], a classifier performs over-confident with its familiar concepts and fear to make predictions for those UNSEEN ones. The calibration issue appears in the generalized few-shot learning as well, *i.e.* SEEN and UNSEEN classifiers have different confidence ranges. We empirically find that directly optimizing two objectives together could not resolve the problem completely.

To this end, we propose *Classifier Synthesis Learning (CASTLE)*, where the few-shot classifiers are synthesized based on a neural dictionary with common characteristics across classes. Such synthesized few-shot classifiers *are then used together* with the many-shot classifiers. To this purpose, we create a scenario, via sampling a set of instances from SEEN categories and pretend that they come from UNSEEN, and apply the synthesized classifiers (based on the instances) as if they are many-shot classifiers to optimize multi-class classification together with the remaining many-shot SEEN classifiers. In other words, we construct few-shot classifiers to *not only perform well on the few-shot classes but also to be competitive when used in conjunction with many-shot classifiers of*

populated classes. We argue that such highly contrastive learning can benefit few-shot classification in two aspects: (1) it provides high discernibility for its synthesized classifiers. (2) it makes the synthesized classifier automatically calibrated with the many-shot classifiers.

Taking steps further, we then propose the *Adaptive Classifier Synthesis Learning* (ACASTLE), with additional flexibility to modify the many-shot classifiers based on few-shot training instances. As a result, it allows backward knowledge transfer [33] — new knowledge learned from novel few-shot training instances can benefit the existing many-shot classifiers. In ACASTLE, the neural dictionary is the concatenation of shared and task-specific neural basis, whose elements summarizes the generality of all visual classes and the specialty of current few-shot categories. This improved neural dictionary facilitates the adaptation of the many-shot classifiers conditioned on the limited “tail” training instances. The adapted many-shot classifiers in ACASTLE *are then used together* with the (jointly) synthesized few-shot classifiers for GFSL classification.

We first verify the effectiveness of the synthesized GFSL classifiers over multi-domain GFSL tasks, where the UNSEEN classes come from diverse domains. ACASTLE can best handle the task heterogeneity due to its ability to adapt the “head” classifiers. Next, we empirically validate our approach on two standard benchmark data sets — *MiniImageNet* and *TieredImageNet*. The proposed approach retains competitive “head” concept recognition performances while outperforming existing approaches on *generalized* few-shot learning with criteria from different aspects. By carefully selecting a prediction bias from the validation set, those miscalibrated FSL approaches perform well in the GFSL scenario. The implicit confidence calibration in CASTLE and ACASTLE works as well as or even better than the post-calibration techniques. We note that CASTLE and ACASTLE could also be used for standard few-shot learning, which outperforms previous state-of-the-art methods when evaluated on benchmarks.

Our contributions are summarized as follows:

- We propose a framework that synthesizes few-shot classifiers for GFSL with a shared neural dictionary, as well as its adaptive variant that modifies SEEN many-shot classifiers to allow the backward knowledge transfer.
- We extend an existing GFSL learning framework into an end-to-end counterpart that learns and contrasts both few-shot and many-shot classifiers simultaneously, which is observed beneficial to the confidence calibration of these two types of classifiers.
- We empirically demonstrate that ACASTLE can back transfer knowledge when learning novel classes with multi-domain GFSL. Meanwhile, we perform a comprehensive evaluation of both ours and existing approaches with various criteria on multiple GFSL benchmarks.

In the rest, we describe the GFSL problem in Section 2, and our CASTLE/ACASTLE approach in Section 3. After that are experimental results, which include setups (Section 4), multi-domain GFSL (Section 5), benchmark GFSL (Section 6.3), analyses (Section 6.4), and standard FSL (Section 6.5). We review related work in Section 7. Finally is the conclusion.

2 Problem Description

We define a K -shot N -way classification task to be one with N classes to make prediction and K training examples per class for learning. The training set (*i.e.*, the support set) is represented as $\mathcal{D}_{\text{train}} = \{(\mathbf{x}_i, \mathbf{y}_i)\}_{i=1}^{NK}$, where $\mathbf{x}_i \in \mathbb{R}^D$ is an instance and $\mathbf{y}_i \in \{0, 1\}^N$ (*i.e.*, one-hot vector) is its label. Similarly, the test set (*a.k.a.* the query set) is $\mathcal{D}_{\text{test}}$, which contains *i.i.d.* samples from the same distribution as $\mathcal{D}_{\text{train}}$.

2.1 From Few-Shot Learning (FSL) to Generalized Few-Shot Learning (GFSL)

In *many-shot learning*, where K is large, a classification model $f : \mathbb{R}^D \rightarrow \{0, 1\}^N$ is learned by optimizing over the instances from the “head” classes:

$$\mathbb{E}_{(\mathbf{x}_i, \mathbf{y}_i) \in \mathcal{D}_{\text{train}}} \ell(f(\mathbf{x}_i), \mathbf{y}_i)$$

Here f is often instantiated as an embedding function $\phi(\cdot) : \mathbb{R}^D \rightarrow \mathbb{R}^d$ and a linear classifier $\Theta \in \mathbb{R}^{d \times N}$: $f(\mathbf{x}_i) = \phi(\mathbf{x}_i)^\top \Theta$. The loss function $\ell(\cdot, \cdot)$ measures the discrepancy between the prediction and the true label.

On the other hand, *Few-shot learning (FSL)* faces the challenge in transferring knowledge across learning visual concepts from “head” to the “tail”. It assumes two non-overlapping sets of SEEN (\mathcal{S}) and UNSEEN (\mathcal{U}) classes. During training, it has access to all SEEN classes for learning an inductive bias, which is then transferred to learn good classifiers on \mathcal{U} rapidly with a small K .

Different from FSL which neglects classification of the \mathcal{S} classes, *Generalized Few-Shot Learning (GFSL)* aims at building a model that simultaneously predicts over $\mathcal{S} \cup \mathcal{U}$ categories. As a result, such a model needs to deal with many-shot classification from $|\mathcal{S}|$ SEEN classes along side with learning $|\mathcal{U}|$ emerging UNSEEN classes.³ In inductive GFSL, the model only has access to the “head” part \mathcal{S} and is required to extract knowledge which facilitates building a joint classifier over SEEN and UNSEEN categories once with limited “tail” examples.

2.2 Meta-learning for few-shot learning

Meta-learning has been an effective framework for FSL [13, 47, 52] in the recent years. The main idea is to *mimic* the future few-shot learning scenario by optimizing a shared f across K -shot N -way tasks drawn from the SEEN class sets \mathcal{S} .

$$\min_f \mathbb{E}_{(\mathcal{D}_{\text{train}}^{\mathcal{S}}, \mathcal{D}_{\text{test}}^{\mathcal{S}}) \sim \mathcal{S}} \mathbb{E}_{(\mathbf{x}_j, \mathbf{y}_j) \in \mathcal{D}_{\text{test}}^{\mathcal{S}}} \left[\ell(f(\mathbf{x}_j; \mathcal{D}_{\text{train}}^{\mathcal{S}}), \mathbf{y}_j) \right] \quad (1)$$

In particular, a K -shot N -way task $\mathcal{D}_{\text{train}}^{\mathcal{S}}$ sampled from \mathcal{S} is constructed by randomly choosing N categories from \mathcal{S} and K examples in each of them.⁴ Following this split use of \mathcal{S} , tasks and classes related to \mathcal{S} are denoted as “meta-training”, and called “meta-val/test” when they are related to \mathcal{U} . A corresponding test set $\mathcal{D}_{\text{test}}^{\mathcal{S}}$ is sampled from the N classes in \mathcal{S} to evaluate the resulting few-shot classifier f . Therefore, we expect the learned classifier f “generalizes” well on the training few-shot tasks sampled from SEEN classes, to “generalize” well on few-shot tasks drawn from UNSEEN class set \mathcal{U} .

Specifically, one popular form of the meta-knowledge to transfer between SEEN and UNSEEN classes is the instance embedding, *i.e.*, $f = \phi$, which transforms input examples into a latent space with d dimensions [47, 52]. ϕ is learned to pull similar objects close while pushing dissimilar ones far away [21]. For a test instance \mathbf{x}_j , the embedding function ϕ makes a prediction based on a soft nearest neighbor classifier:

$$\begin{aligned} \hat{y}_j &= f(\mathbf{x}_j; \mathcal{D}_{\text{train}}) \\ &= \sum_{(\mathbf{x}_i, \mathbf{y}_i) \in \mathcal{D}_{\text{train}}} \text{sim}(\phi(\mathbf{x}_j), \phi(\mathbf{x}_i)) \cdot \mathbf{y}_i \end{aligned}$$

$\text{sim}(\phi(\mathbf{x}_j), \phi(\mathbf{x}_i))$ measures the similarity between the test instance $\phi(\mathbf{x}_j)$ and each training instance $\phi(\mathbf{x}_i)$. When there is more than one instance per class, *i.e.*, $K > 1$, instances in the same class can be averaged to assist make a final decision. By learning a good ϕ , important visual features for few-shot classification are distilled, which helps the few-shot tasks with classes from the UNSEEN classes.

3 Method

The main idea of CASTLE and ACASTLE includes an effective learning algorithm that learns many-shot classifiers and few-shot classifiers at the same time, and a classifier composition model for synthesizing classifiers with the few-shot training data in an end-to-end manner. In Section 3.1, we utilize a unified learning objective that directly contrasts many-shot classifiers with few-shot classifiers, via constructing classification tasks over $\mathcal{U} \cup \mathcal{S}$ categories. By reusing the parameters of the many-shot classifier, the learned model calibrates the prediction ranges over “head” and “tail” classes naturally. It enforces the few-shot classifiers to explicitly compete against the many-shot classifiers in the model learning, which leads to more discriminative few-shot classifiers in the GFSL setting. In Section 3.2, we introduce the classifier composition model uses a few-shot training data to query the neural bases, and then assemble the target “synthesized classifiers”. CASTLE sets a shared neural bases across tasks, which keeps stationary many-shot classifiers all the time; while with both

³ $|\mathcal{S}|$ and $|\mathcal{U}|$ denote the total number of classes from the SEEN and UNSEEN class sets respectively.

⁴We use the super-script \mathcal{S} and \mathcal{U} to denote a set or an instance sampled from \mathcal{S} and \mathcal{U} respectively.

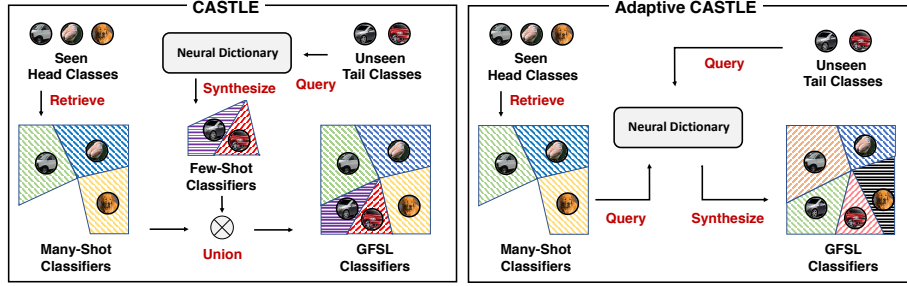


Figure 2: Illustration of adaptive GFSL learning process of CASTLE and ACASTLE. Different from the stationary learning process (l.h.s.) of CASTLE, ACASTLE (r.h.s.) synthesizes the GFSL classifiers for SEEN and UNSEEN classes in an adaptive manner – the many-shot classifiers of “head” classes are also conditioned on the training instances from the “tail” classes.

shared and specific components in the neural dictionary, the SEEN class classifiers will be adapted based on its relationship with UNSEEN class instances in ACASTLE.

3.1 Unified Learning of Few-Shot and Many-Shot Classifiers

In addition to transferring knowledge from SEEN to UNSEEN classes as in FSL, in generalized few-shot learning, the few-shot classifiers is required to do well when used in conjunction with many-shot classifiers. Therefore, a GFSL classifier f should have a low expected error as what follows:

$$\mathbb{E}_{\mathcal{D}_{\text{train}}^{\mathcal{U}}} \mathbb{E}_{(\mathbf{x}_j, \mathbf{y}_j) \in \mathcal{D}_{\text{test}}^{\mathcal{S} \cup \mathcal{U}}} \left[\ell \left(f \left(\mathbf{x}_j; \mathcal{D}_{\text{train}}^{\mathcal{U}}, \Theta_{\mathcal{S}} \right), \mathbf{y}_j \right) \right] \quad (2)$$

Suppose we have sampled a K -shot N -way few-shot learning task $\mathcal{D}_{\text{train}}^{\mathcal{U}}$, which contains $|\mathcal{U}|$ visual UNSEEN categories. For each task, the classifier f predicts a test instance in $\mathcal{D}_{\text{test}}^{\mathcal{S} \cup \mathcal{U}}$ towards *both* tail classes \mathcal{U} and head classes \mathcal{S} . In other words, based on $\mathcal{D}_{\text{train}}^{\mathcal{U}}$ and the token of the many-shot classifiers $\Theta_{\mathcal{S}}$, a randomly sampled instance in $\mathcal{S} \cup \mathcal{U}$ should be effectively predicted. In summary, a GFSL classifier generalizes its joint prediction ability to $\mathcal{S} \cup \mathcal{U}$ given $\mathcal{D}_{\text{train}}^{\mathcal{U}}$ and $\Theta_{\mathcal{S}}$ during inference.

Unified learning objective. ACASTLE learns a generalizable GFSL classifier via training on the SEEN class set \mathcal{S} . For each class in $s \in \mathcal{S}$, it keeps a many-shot classifier (*i.e.*, liner classifier over the embedding function $\phi(\cdot)$) Θ_s . The token set $\Theta_{\mathcal{S}}$ summarizes the information to classifier the SEEN classes \mathcal{S} , and we set it as the union of the liner classifiers $\{\Theta_s\}$.

Next, we sample a “fake” K -shot N -way few-shot task from \mathcal{S} , which contains \mathcal{C} categories. Given the “fake” few-shot task, we treat the remaining $\mathcal{S} - \mathcal{C}$ classes as the “fake” head classes, whose corresponding many-shot classifiers tokens are $\Theta_{\mathcal{S}-\mathcal{C}}$. Then the GFSL model needs to build classifiers target any instance in $\mathcal{C} \cup (\mathcal{S} - \mathcal{C})$. We synthesize both the few-shot classifiers for \mathcal{C} by $\mathbf{W}_{\mathcal{C}} = \{ \mathbf{w}_c \mid c \in \mathcal{C} \}$ and the many-shot classifiers $\hat{\Theta}_{\mathcal{S}-\mathcal{C}} = \{ \hat{\Theta}_c \mid c \in \mathcal{S} - \mathcal{C} \}$ with a neural dictionary, so that the composition of one classifier will takes the context of others into account. The details of the neural dictionary will be described in the next subsection.

Both the synthesized many-shot classifiers (from the “fake” many-shot classes $\mathcal{S} - \mathcal{C}$) $\hat{\Theta}_{\mathcal{S}-\mathcal{C}}$ and few-shot classifiers (from the “fake” few-shot classes \mathcal{C}) $\mathbf{W}_{\mathcal{C}}$ are combined together to form the set of joint classifiers $\hat{\mathbf{W}} = \mathbf{W}_{\mathcal{C}} \cup \hat{\Theta}_{\mathcal{S}-\mathcal{C}}$, over *all* classes in \mathcal{S} .

Finally, we optimize the learning objective as follows:

$$\min_{\{\phi, \mathbf{B}, \{\Theta_s\}, \mathcal{U}, \mathcal{V}\}} \sum_{\mathcal{C} \subset \mathcal{S}} \sum_{(\mathbf{x}_j, \mathbf{y}_j) \sim \mathcal{S}} \ell \left(\hat{\mathbf{W}}^{\top} \phi(\mathbf{x}_j), \mathbf{y}_j \right) \quad (3)$$

Despite that the few-shot classifiers $\mathbf{W}_{\mathcal{C}}$ are synthesized using with K training instances, they are optimized to perform well on all the instances from \mathcal{C} and moreover, to perform well against all the instances from other SEEN categories. The many-shot classifiers $\Theta_{\mathcal{S}}$ are not stationary, which are *adapted* based on the context of the current few-shot instances (the adaptive GFSL classifier notion

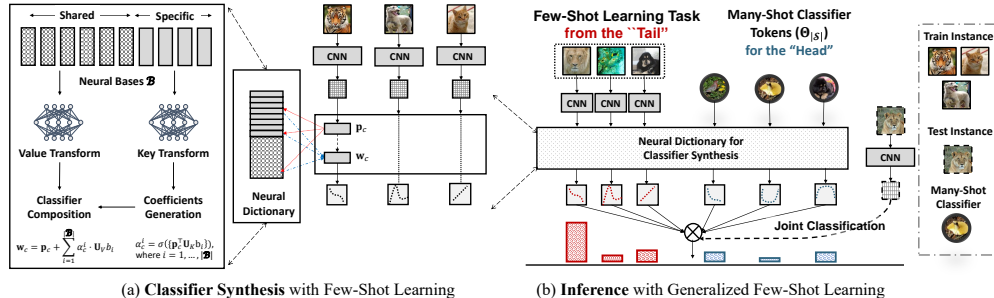


Figure 3: Illustration of Adaptive Classifier Synthesize Learning (ACASTLE). A neural dictionary contains two types of neural bases – the shared component and the task-specific component. During the inference, both the prototype of the “tail” classes and the token of the SEEN classifiers are input into the neural dictionary, and synthesize the joint classifiers over both SEEN and UNSEEN categories.

is illustrated in Figure 2). Note that \mathbf{W}_C and $\hat{\Theta}_{S-C}$ are synthesized based on the neural dictionary, which serves as the **bridge** to connect \mathcal{C} (few-shot) and $(\mathcal{S} - \mathcal{C})$ (many-shot).

After minimizing the accumulated loss in Eq. 3 over multiple GFSL tasks, the learned model extends its discerning ability to UNSEEN classes so as has low error in Eq. 2. During inference, ACASTLE synthesizes the classifiers for UNSEEN classes based on the neural dictionary with their few-shot training examples, and makes a joint prediction over $\mathcal{S} \cup \mathcal{U}$ with the help of the *adapted* many-shot classifier $\hat{\Theta}_S$.

Reuse Many-Shot Classifiers. We optimize Eq. 3 using the many-shot classifier over \mathcal{S} to initialize the embedding ϕ . In detail, a $|\mathcal{S}|$ -way many-shot classifier is trained over all SEEN classes with the cross-entropy loss, whose backbone is used to initialize the embedding ϕ in the GFSL classifier. We empirically observed that such initialization is essential for the prediction calibration between SEEN and UNSEEN classes, more details could be found in Section 6.4.

Multi-classifier learning. A natural way to minimize Eq. 3 implements a stochastic gradient descent step in each mini-batch by sampling one GFSL task, which contains a K -shot N -way training set together with a set of test instances $(\mathbf{x}_j, \mathbf{y}_j)$ from \mathcal{S} . It is clear that increasing the number of GFSL tasks per gradient step can improve the optimization stability. Therefore, we propose an efficient implementation that utilizes *a large number of* GFSL tasks to compute gradients. Specifically, we sample two sets of instances from *all* SEEN classes, *i.e.*, $\mathcal{D}_{\text{train}}^S$ and $\mathcal{D}_{\text{test}}^S$. Then we construct a large number of joint classifiers $\{\hat{\mathbf{W}}^z = \mathbf{W}_C^z \cup \hat{\Theta}_{S-C}^z \mid z = 1, \dots, Z\}$ with different sets of \mathcal{C} , which is then applied to compute the averaged loss over z using Eq. 3. In the scope of this paper, ACASTLE variants always use *multi-classifier learning* unless it is explicitly mentioned. With this, we observed a significant speed-up in terms of convergence (cf. Section 6.4 for an ablation study).

3.2 Classifier Composition with a Neural Dictionary

We use neural dictionary to implement the prediction $f(\mathbf{x}_j; \mathcal{D}_{\text{train}}^U, \Theta_S)$ in Eq. 2. To classify an instance during inference, both the limited “tail” instances $\mathcal{D}_{\text{train}}^U$ and the context of the SEEN classifiers tokens Θ_S are taken into account. We describe the composition of the neural dictionary and the way to synthesize “tail” classifiers first, followed by the adaption of the “head” classifiers. The neural dictionary formalizes both “head” and “tail” classifiers with common bases, which benefits the relationship transition between classes. Furthermore, the neural dictionary encodes the shared primitives for composing classifiers, which serves as a kind of meta-knowledge to be transferred across both the SEEN and the UNSEEN classes.

Here we define a neural dictionary as pairs of learnable “key” and “value” embeddings, where each “key” and “value” is associated with a set of neural bases, which are designed to encode shared primitives for composing classifiers of $\mathcal{S} \cup \mathcal{U}$. Formally, the neural bases contain two sets of elements:

$$\mathcal{B} = \mathcal{B}_{\text{share}} \cup \mathcal{B}_{\text{specific}}$$

$\mathcal{B}_{\text{share}}$ contains a set of $|\mathcal{B}_{\text{share}}|$ learnable bases $\mathcal{B}_{\text{share}} = \{\mathbf{b}_1, \mathbf{b}_2, \dots, \mathbf{b}_{|\mathcal{B}_{\text{share}}|}\}$, and $\mathbf{b}_k \in \mathcal{B}_{\text{share}} \in \mathbb{R}^d$. This part in the neural dictionary is shared when synthesizing classifiers for different kinds of tasks. $\mathcal{B}_{\text{specific}}$ characterizes the local information of the input to the neural dictionary, *i.e.*, the training set $\mathcal{D}_{\text{train}}$ of the current few-shot task with “tail” classes and the tokens of the many-shot classifiers.

The key and value for the neural dictionary are generated based on two linear projections U and V of elements in the bases \mathcal{B} . For instance, $U\mathbf{b}_k$ and $V\mathbf{b}_k$ represent the generated key and value embeddings. For a query to the neural dictionary, it first computes similarity with all keys ($U\mathbf{b}_k$), and the corresponding output of the query is the combination of the computed similarity with all elements in the value set ($V\mathbf{b}_k$).

In a “fake” K -shot N -way few-shot task from \mathcal{S} , there are \mathcal{C} categories. Denote $\mathbb{I}[y_i = c]$ as an indicator that selects instances in the class c . To synthesize a classifier for a class c , we first compute the class signature as the embedding prototype, defined as the average embedding of all K shots of instances (in a K -shot N -way task):⁵

$$\mathbf{p}_c = \frac{1}{K} \sum_{(\mathbf{x}_i, y_i) \in \mathcal{D}_{\text{train}}} \phi(\mathbf{x}_i) \cdot \mathbb{I}[y_i = c] \quad (4)$$

The specific component in the neural dictionary bases \mathcal{B} is the concatenation of the prototype of few-shot instances $\{\mathbf{p}_c\}$ and the linear classifiers token set $\Theta_{\mathcal{S}-\mathcal{C}}$ over the embedding ϕ , *i.e.*,

$$\mathcal{B}_{\text{specific}} = \{\mathbf{p}_c \mid c \in \mathcal{C}\} \cup \Theta_{\mathcal{S}-\mathcal{C}}$$

We then compute the coefficients α_c for assembling the classifier of class c , via measuring the compatibility score between the class signature and the key embeddings of the neural dictionary,

$$\alpha_c^k \propto \exp(\mathbf{p}_c^\top U\mathbf{b}_k), \text{ where } k = 1, \dots, |\mathcal{B}|$$

The coefficient α_c^k is then *normalized* with the sum of compatibility scores over all $|\mathcal{B}|$ bases, which then is used to convexly combine the value embeddings and synthesize the classifier,

$$\mathbf{w}_c = \mathbf{p}_c + \sum_{k=1}^{|\mathcal{B}|} \alpha_c^k \cdot V\mathbf{b}_k \quad (5)$$

We formulate the classifier composition as a summation of the initial prototype embedding \mathbf{p}_c and the residual component $\sum_{k=1}^{|\mathcal{B}|} \alpha_c^k \cdot U_V\mathbf{b}_k$. Such a composed classifier is then ℓ_2 -normalized and used for (generalized) few-shot classification. The same classifier synthesize process could be applied to the elements in SEEN class token set $\Theta_{\mathcal{S}-\mathcal{C}}$, where a “head” classifier first compute similarity with the shared neural bases and the “tail” prototypes, then adapt the classifier to $\hat{\Theta}_{\mathcal{S}-\mathcal{C}}$ with Eq. 5. Therefore, the SEEN classifiers are also synthesized conditioned on the context of the UNSEEN instances, which promotes the backward knowledge transfer from UNSEEN classes to the SEEN ones.

Since both the embedding “key” and classifier “value” are generated based on the same set of neural bases, it encodes a compact set of latent features for a wide range of classes in $\mathcal{B}_{\text{share}}$ while leaving the task-specific characteristic in $\mathcal{B}_{\text{specific}}$. We hope the learned neural bases contain a rich set of classifier primitives to be transferred to novel compositions of emerging visual categories. Figure 3 demonstrates the classifier synthesize process with the neural dictionary.

We denote the degenerated version with only the shared neural bases $\mathcal{B} = \mathcal{B}_{\text{share}}$ as CASTLE, which makes a joint prediction with the stationary many-shot classifier $\Theta_{\mathcal{S}}$ and the synthesized few-shot classifiers.

Remark. Changpinyo *et al* [6, 7] take advantage of the dictionary to synthesize the classifiers for all classes in zero-shot learning. Gidaris and Komodakis [15] implement a GFSL model with two stages. After pre-training a many-shot classifier, it freezes the embedding and composes the “tail” classifiers by convex combinations of the transforms of the “head” classifiers. Different from the previous approach constructing a dictionary based on a pre-fixed feature embedding, we use a *learned* embedding function together with the neural dictionary, leading to an end-to-end GFSL framework.

⁵More choices of Eq. 4 are investigated in Section 6.4.

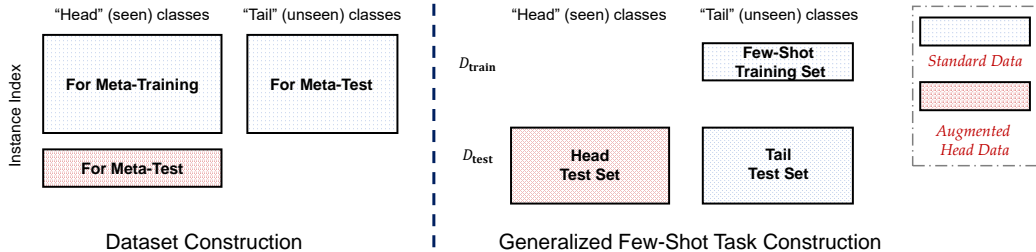


Figure 4: The split of data in the generalized few-shot classification scenario. In addition to the standard data set like *MiniImageNet* (blue part), we collect non-overlapping augmented “head” class instances from the corresponding categories in the ImageNet (red part), to measure the classification ability on the seen classes. Then in the generalized few-shot classification task, few-shot instances are sampled from each of the unseen classes, while the model should have the ability to predict instances from *both* the “head” and “tail” classes.

Furthermore, different from [15] keeping the “head” classifiers stationary, we adapt them conditioned on the “tail” classes, which could handle the diversity between class domains (as illustrated in Figure 2). Comprehensive experiments to verify the effectiveness of such adaptive GFSL classifiers could be found in Section 5 and Section 6.3.

4 Experimental Setups

This section details the experimental setups, including the general data splits strategy, the pre-training technique, the specifications of the feature backbone, and the evaluation metrics for GFSL.

4.1 Data Splits

We visualize the general data split strategy in Figure 4. There are two parts of data set for standard meta-learning tasks. The meta-training set for model learning (corresponds to the SEEN classes), and the meta-val/test part for model evaluation (corresponds to the UNSEEN classes). To evaluate a GFSL model, we’d like to augment the meta-training set with new instances, so that the classification performance on SEEN classes could be measured. During the inference phase, a few-shot training set from UNSEEN classes are provided with the model, and the model should make a joint prediction over instances from *both* the “head” and “tail” classes. We will describe the detailed splits for particular data sets in later sections.

4.2 Pre-training Strategy

Before the meta-training stage, we try to find a good initialization for the embedding ϕ . In particular, on *MiniImageNet*, we add a linear layer on the backbone output and optimize a 64-way classification problem on the meta-training set with the cross-entropy loss function. Stochastic gradient descent with initial learning rate 0.1 and momentum 0.9 is used to complete such optimization. The 16 classes in *MiniImageNet* for model selection also assist the choice of the pre-trained model. After each epoch, we use the current embedding and measures the nearest neighbor based few-shot classification performance on the sampled few-shot tasks from these 16 classes. The most suitable embedding function is recorded. After that, such a learned backbone is used to initialize the embedding part ϕ of the whole model. The same strategy is also applied on the meta-training set of the *TieredImageNet*, *Heterogeneous*, and *Office-Home* data sets, where a 351-way, 100-way, and 25-way classifiers are pre-trained.

In later sections (cf. Section 6.4), we will verify this pre-training strategy does not influence the few-shot classification performance a lot, but it is essential to make the GFSL classifier well-calibrated.

4.3 Feature Network Specification

Following the setting of most recent methods [37, 44, 60], we use ResNet-12 [4, 18] to implement the embedding backbone ϕ . Different from the standard configuration, the literature [37, 44, 60] resize

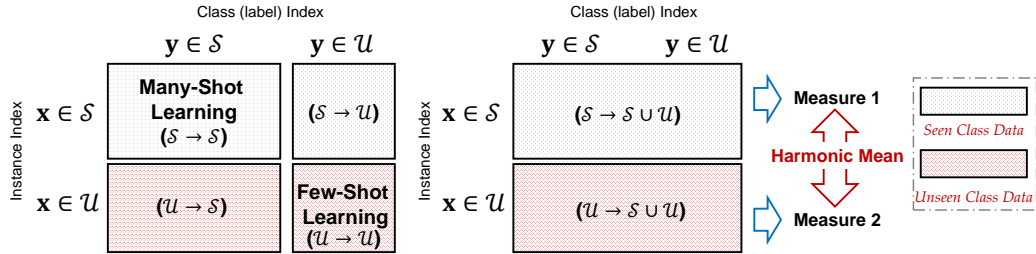


Figure 5: An illustration of the harmonic mean based criterion for GFSL evaluation. \mathcal{S} and \mathcal{U} denotes the SEEN and UNSEEN instances (\mathbf{x}) and labels (\mathbf{y}) respectively. $\mathcal{S} \cup \mathcal{U}$ is the joint set of \mathcal{S} and \mathcal{U} . The notation $X \rightarrow Y, X, Y \in \{\mathcal{S}, \mathcal{U}, \mathcal{S} \cup \mathcal{U}\}$ means computing prediction results with instances from X to labels of Y . By computing a performance measure (like accuracy) on the joint label space prediction of SEEN and UNSEEN instances separately, a harmonic mean is computed to obtain the final measure.

the input image to $80 \times 80 \times 3$ for *MiniImageNet* (while $84 \times 84 \times 3$ for *TieredImageNet* and other data sets) and remove the first two down-sampling layers in the network. In concrete words, three residual blocks are used after an initial convolutional layer (with stride 1 and padding 1) over the image, which have channels 160/320/640, stride 2, and padding 2. After a global average pooling layer, it leads to a 640 dimensional embedding.

We use the pre-trained backbone to initialize the embedding part ϕ of a model for CASTLE/ACASTLE and our re-implemented comparison methods such as MC+ k NN, ProtoNet+ProtoNet, MC+ProtoNet, L2ML [58], and DFSL [15].⁶ When there exists a backbone initialization, we set the initial learning rate as $1e-4$ and optimize the model with Momentum SGD. The learning rate will be halved after optimizing 2,000 mini-batches. During meta-learning, all methods are optimized over 5-way few-shot tasks, where the number of shots in a task is consistent with the inference (meta-test) stage. For example, if the goal is a 1-shot 5-way model, we sample 1-shot 5-way $\mathcal{D}_{\text{train}}^{\mathcal{S}}$ during meta-training, together with 15 instances per class in $\mathcal{D}_{\text{test}}^{\mathcal{S}}$.

For CASTLE/ACASTLE, we take advantage of the multi-classifier training technique to improve the learning efficiency. We randomly sample a 24-way task from \mathcal{S} in each mini-batch, and re-sample 64 5-way tasks from it. It is notable that all instances in the 24-way task are encoded by the ResNet backbone with the same parameters in advance. Therefore, by embedding the synthesized 5-way few-shot classifiers into the global many-shot classifier, it results in 64 different configurations of the generalized few-shot classifiers. To evaluate which we randomly sample instances with batch size 128 from \mathcal{S} and compute the GFSL objective in Eq. 3.⁷

4.4 Evaluation Measures

We take advantage of the auxiliary meta-training set from the benchmark data sets during GFSL evaluations, and an illustration of the data set construction can be found in Figure 4. The notation $X \rightarrow Y$ with $X, Y \in \{\mathcal{S}, \mathcal{U}, \mathcal{S} \cup \mathcal{U}\}$ means computing prediction results with instances from X to labels of Y . For example, $\mathcal{S} \rightarrow \mathcal{S} \cup \mathcal{U}$ means we first filter instances come from the SEEN class set ($\mathbf{x} \in \mathcal{S}$), and predict them into the joint label space ($\mathbf{y} \in \mathcal{S} \cup \mathcal{U}$). For a GFSL model, we consider its performance with different measurements.

Few-shot accuracy. Following the standard protocol [13, 47, 52, 60], we sample 10,000 K -shot N -way tasks from \mathcal{U} during inference. In detail, we first sample N classes from \mathcal{U} , and then sample $K + 15$ instances for each class. The first NK labeled instances (K instances from each of the N classes) are used to build the few-shot classifier, and the remaining $15N$ (15 instances from each of the N classes) are used to evaluate the quality of such few-shot classifier. During our test, we consider $K = 1$ and $K = 5$ as in the literature, and change N ranges from $\{5, 10, 15, \dots, |\mathcal{U}|\}$ as a

⁶Details of the comparison methods and baselines are in the later subsections.

⁷Our implementation will be publicly available on <https://github.com/Shalab/CASTLE>

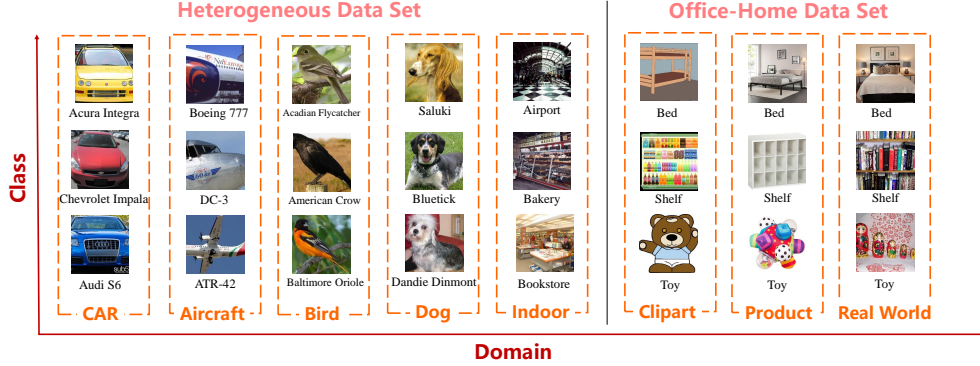


Figure 6: An illustration of the Heterogeneous and Office-Home dataset. Both datasets contain multiple domains. In the Heterogeneous dataset, each class belongs to only one domain, while in Office-Home, a class has images from all three domains.

more robust measure. It is noteworthy that in this test stage, all the instances come from \mathcal{U} and are predicted to classes in \mathcal{U} ($\mathcal{U} \rightarrow \mathcal{U}$).

Generalized few-shot accuracy. Different from many-shot and few-shot evaluations, the generalized few-shot learning takes the joint instance and label spaces into consideration. In other words, the instances come from $\mathcal{S} \cup \mathcal{U}$ and their predicted labels also in $\mathcal{S} \cup \mathcal{U}$ ($\mathcal{S} \cup \mathcal{U} \rightarrow \mathcal{S} \cup \mathcal{U}$). This is obviously more difficult than the many-shot ($\mathcal{S} \rightarrow \mathcal{S}$) and few-shot ($\mathcal{U} \rightarrow \mathcal{U}$) tasks. During the test, with a bit abuse of notations, we sample K -shot $\mathcal{S} + N$ -way tasks from $\mathcal{S} \cup \mathcal{U}$. Concretely, we first sample a K -shot N -way task from \mathcal{U} , with NK training and $15N$ test instances respectively. Then, we randomly sample $15N$ instances from \mathcal{S} . Thus in a GFSL evaluation task, there are NK labeled instances from \mathcal{U} , and $30N$ test instances from $\mathcal{S} \cup \mathcal{U}$. We compute the accuracy of $\mathcal{S} \cup \mathcal{U}$ as the final measure. We abbreviate this criterion as “Mean Acc.” or “Acc.” in later sections.

Generalized few-shot Δ -value. Since the problem becomes difficult when the predicted label space expands from $\mathcal{S} \rightarrow \mathcal{S}$ to $\mathcal{S} \rightarrow \mathcal{S} \cup \mathcal{U}$ (and also $\mathcal{U} \rightarrow \mathcal{U}$ to $\mathcal{U} \rightarrow \mathcal{S} \cup \mathcal{U}$), the accuracy of a model will have a drop. To measure how the classification ability of a GFSL model changes when working in a GFSL scenario, Ren *et al.* [41] propose the Δ -Value to measure the average accuracy drop. In detail, for each sampled GFSL task, we first compute its many-shot accuracy ($\mathcal{S} \rightarrow \mathcal{S}$) and few-shot accuracy ($\mathcal{U} \rightarrow \mathcal{U}$). Then we calculate the corresponding accuracy of SEEN and UNSEEN instances in the joint label space, *i.e.*, $\mathcal{S} \rightarrow \mathcal{S} \cup \mathcal{U}$ and $\mathcal{U} \rightarrow \mathcal{S} \cup \mathcal{U}$. The Δ -Value is the average decrease of accuracy in these two cases. We abbreviate this criterion as “ Δ -value” in later sections.

Generalized few-shot harmonic mean. Directly computing the accuracy still gets biased towards the populated classes, so we also consider the harmonic mean as a more balanced measure [59]. By computing performance measurement such as top-1 accuracy for $\mathcal{S} \rightarrow \mathcal{S} \cup \mathcal{U}$ and $\mathcal{U} \rightarrow \mathcal{S} \cup \mathcal{U}$, the harmonic mean is used to average the performance in these two cases as the final measure. An illustration is in Figure 5. We abbreviate this criterion as “HM” or “HM Acc.” in later sections.

Generalized few-shot AUSUC. Chao *et al.* [9] propose a calibration-agnostic criterion for generalized zero-shot learning. To avoid evaluating a model influenced by a calibration factor between SEEN and UNSEEN classes, they propose to determine the range of the calibration factor for all instances at first, and then plot the SEEN-UNSEEN accuracy curve based on different configurations of the calibration values. Finally, the area under the SEEN-UNSEEN curve is used as a more robust criterion. We follow [9] to compute the AUSUC value for sampled GFSL tasks. We abbreviate this criterion as “AUSUC” in later sections.

5 Pivot Study on Multi-Domain GFSL

We first present a pivot study to demonstrate the effectiveness of ACASTLE, which leverages adaptive classifiers synthesized for both SEEN and UNSEEN classes. To achieve this, we investigate two multi-domain datasets – “Heterogeneous” and “Office-Home” with more challenging settings, where

Table 1: Generalized 1-shot classification performance (mean accuracy and harmonic mean accuracy) on (a) the Heterogeneous dataset with **100 Head and 5 Tail categories** and (b) the Office-Home dataset with **25 Head and 5 Tail categories**. $\mathcal{S} \rightarrow \mathcal{S} \cup \mathcal{U}$ and $\mathcal{U} \rightarrow \mathcal{S} \cup \mathcal{U}$ denote the joint classification accuracy for SEEN class and UNSEEN class instances respectively. CASTLE⁻ is the variant of CASTLE without using the neural dictionary.

(a) Heterogeneous dataset					(b) Office-Home dataset				
Measures	$\mathcal{S} \cup \mathcal{U} \rightarrow \mathcal{S} \cup \mathcal{U}$	$\mathcal{S} \rightarrow \mathcal{S} \cup \mathcal{U}$	$\mathcal{U} \rightarrow \mathcal{S} \cup \mathcal{U}$	HM Acc.	Measures	$\mathcal{S} \cup \mathcal{U} \rightarrow \mathcal{S} \cup \mathcal{U}$	$\mathcal{S} \rightarrow \mathcal{S} \cup \mathcal{U}$	$\mathcal{U} \rightarrow \mathcal{S} \cup \mathcal{U}$	HM Acc.
DFSL [15]	48.13 \pm 0.12	46.33 \pm 0.12	48.25 \pm 0.22	47.27 \pm 0.12	DFSL [15]	35.72 \pm 0.12	28.42 \pm 0.12	39.77 \pm 0.22	33.15 \pm 0.12
CASTLE ⁻	48.29 \pm 0.12	45.13 \pm 0.13	50.14 \pm 0.22	47.50 \pm 0.12	CASTLE ⁻	35.74 \pm 0.13	27.93 \pm 0.13	42.59\pm0.22	33.73 \pm 0.13
CASTLE	50.16 \pm 0.13	48.05 \pm 0.13	50.86\pm0.22	49.05 \pm 0.12	CASTLE	35.77 \pm 0.13	29.03 \pm 0.13	42.46 \pm 0.22	34.48 \pm 0.13
ACASTLE	53.01\pm0.12	56.18\pm0.12	49.84 \pm 0.22	52.81\pm0.13	ACASTLE	39.99\pm0.14	40.29\pm0.13	39.68 \pm 0.22	39.98\pm0.14

a GFSL model is required to *transfer knowledge in backward direction* (adapt SEEN classifiers based on UNSEEN ones) to obtain superior joint classification performances over heterogeneous domains.

5.1 Dataset

We construct a **Heterogeneous** dataset based on 5 fine-grained classification datasets, namely Air-Craft [34], Car-196 [22], Caltech-UCSD Birds (CUB) 200-2011 [54], Stanford Dog [20], and Indoor Scenes [38]. Since images in the sub-datasets have apparent heterogeneous semantics, we treat images from different fine-grained datasets as different domains. 20 classes with 50 images in each of them are randomly sampled from each of the 5 datasets to construct the meta-training set. The same sampling strategy is also used to sample classes for model validation (meta-val) and evaluation (meta-test) sets. Therefore, there are 100 classes for meta-training/val/test sets, which contains 20 classes from each fine-grained dataset. To evaluate the performance of a GFSL model, we augment the meta-training set by sampling another 15 images from the corresponding classes for each of the SEEN classes⁸.

We also investigate the **Office-Home** [51] dataset, which originates from a domain adaptation task. There are 65 classes and 4 domains of images per class. Considering the scarce number of images in one particular domain, we select three of the four domains, “Clipart”, “Product”, and “Real World” to construct our dataset. The number of instances in a class per domain is not equal. We randomly sample 25 classes (with all selected domains) for meta-training, 15 classes for meta-validation, and the remaining 25 classes are used for meta-test. Similarly, we hold out 10 images per domain for each SEEN classes to evaluate the generalized classification ability of a GFSL model.

Note that in addition to the class label, images in these two datasets are also equipped with *at least one* domain label. In particular, classes in Heterogeneous dataset belong to a single domain corresponding to “aircraft”, “bird”, “car”, “dog”, or “indoor scene”, while the classes in Office-Home possess images from all 3 domains, namely “Clipart”, “Product” and “Real World”. An illustration of the sampled images (of different domains) from these two datasets are shown in Figure 6.

The key difference to standard GFSL (cf. Section 6.3) is that here the SEEN categories are collected from multiple (heterogeneous) visual domains and used for training the inductive GFSL model. During the evaluation, the few-shot training instances of “tail” classes *only come from one single domain*. With this key difference, we note that the UNSEEN few-shot classes are close to a certain sub-domain of SEEN classes and relatively far away from the others. Therefore, a model capable of adapting its SEEN classifiers can take the advantages and adapt itself to the domain of the UNSEEN classes.

5.2 Baselines and Comparison Methods

Besides CASTLE and ACASTLE, we consider two other baseline models. The first one optimizes the Eq. 3 directly but without the neural dictionary, which relies on both the (fixed) linear classifier $\Theta_{\mathcal{S}}$ and the few-shot prototypes to make a GFSL prediction (we denote it as “CASTLE⁻”); the second one is DFSL [15], which requires a two-stage training of the GFSL model. It trains a many-shot classifier with cosine similarity in the first stage. Then it freezes the backbone model as feature extractor and optimizes a similar form of Eq. 3 via composing new few-shot classifiers as the convex combination of those many-shot classifiers. It can be viewed as a degenerated neural dictionary,

⁸We will release the dataset and pre-processing code for reproducibility

where DFSL sets a size- $|\mathcal{S}|$ “shared” bases $\mathcal{B}_{\text{share}}$ as the many-shot classifier $\Theta_{\mathcal{S}}$. We observe that DFSL is unstable to perform end-to-end learning. It is potentially because the few-shot classifier composition uses many-shot classifiers as bases, but those bases are optimized to both be good bases and good classifiers, which can likely to be conflicting to some degree. It is also worth noting that all the baselines except ACASTLE only modifies to the few-shot classifiers and it is impossible for them to perform backward knowledge transfer.

5.3 GFSL over Heterogeneous Dataset

The Heterogeneous dataset has 100 SEEN classes in the meta-training set, 20 per domain. We consider the case where during the inference, all of the “tail” classes come from one particular domain. For example, the “tail” classes are different kinds of birds, and we need to do a joint classification over all SEEN classes from the heterogeneous domains and the newly coming “tail” classes with limited instances. To mimic the inference scenario, we sample “fake” few-shot tasks with classes from one of the five domains randomly, and contrasting the discerning ability from the sampled classes w.r.t. the remaining SEEN classes as in Eq. 3.

Note that we train DFSL strictly follows the strategy in [15], and train other GFSL models with a pre-trained embedding and the multi-classifier techniques to improve the training efficiency. Following [15, 45, 59], we compute the 1-Shot 5-Way GFSL classification mean accuracy and harmonic mean accuracy over 10,000 sampled tasks, whose results are recorded in Table 1. $\mathcal{S} \rightarrow \mathcal{S} \cup \mathcal{U}$ and $\mathcal{U} \rightarrow \mathcal{S} \cup \mathcal{U}$ denote the average accuracy for the joint prediction of SEEN and UNSEEN instances respectively.

From the results in Table 1, DFSL could not work well due to its fixed embedding and restricted bases. CASTLE⁻ is able to balance the training accuracy of both SEEN and UNSEEN classes benefited from the pre-train strategy and the unified learning objective, which achieves the highest joint classification performance over UNSEEN classes. The discriminative ability is further improved with the help of the neural dictionary. CASTLE performs better than its degenerated version, which verifies the effectiveness of the learned neural bases. The neural dictionary encodes the common characteristic among all classes for the GFSL classification, so that CASTLE gets better mean accuracy and harmonic mean accuracy than CASTLE⁻. Since ACASTLE is able to adapt both many-shot and few-shot classifiers conditioned on the context of the “tail” instances, it obtains the best GFSL performance in this case. It is notable that ACASTLE gets much higher joint classification accuracy for SEEN classes than other methods, which validates its ability to adapt the many-shot classifier over the SEEN classes based on the context of “tail” classes.

5.4 GFSL over Office-Home Dataset

We also investigate the similar multi-domain GFSL classification task over the Office-Home dataset. However, in this case, a single class could belong to all three domains. We consider the scenario to classify classes in a single domain and the domain of the classes should be inferred from the limited “tail” instances. In other words, we train a GFSL model over 25 classes, and each class has 3 sets of instances corresponding to the three domains. In meta-training, a 25-way SEEN class classifier is constructed. During the inference, the model is provided by another 5-way 1-shot set of UNSEEN class instances from one single domain. The model is required to output a joint classifier for test instances from the whole 30 classes whose domains are the same as the one in the UNSEEN class set.

Towards such a multi-domain GFSL task, we train a GFSL model by keeping the instances in both the few-shot fake “tail” task and corresponding test set from the same domain. We use the same set of comparison methods and evaluation protocols with the previous subsection. The mean accuracy, harmonic mean accuracy, and the specific accuracy for SEEN and UNSEEN classes are shown in Table 1.

Due to the ambiguity of domains for each class, the GFSL classification over Office-Home gives rise to a more difficult problem, while the results in Table 1 reveal a similar trend with those in Table 1. Since for Office-Home a single GFSL model needs to make the joint prediction over classes from multiple domains conditioned on different configurations of the “tail” few-shot tasks, the stationary SEEN class classifiers are not suitable for the classification over different domains. In this case, ACASTLE still achieves the best performance over different GFSL criteria, and gets larger superiority margins with the comparison methods.

6 Experiments on GFSL

In this section, we design experiments on benchmark datasets to validate the effectiveness of the CASTLE and ACASTLE in GFSL (cf. Section 6.3). After a comprehensive comparison with competitive methods using various protocols, we analyze different aspects of GFSL approaches (cf. Section 6.4), and we observe the post calibration makes the FSL methods strong GFSL baselines. We verify that CASTLE/ACASTLE learn a better calibration between SEEN and UNSEEN classifiers, and the neural dictionary makes CASTLE/ACASTLE persist its high discerning ability with incremental “tail” few-shot instances. Finally, we show that CASTLE/ACASTLE also benefit standard FSL performances (cf. Section 6.5).

6.1 Datasets

Two benchmark datasets are used in our experiments. The *MiniImageNet* dataset [52] is a subset of the ILSVRC-12 dataset [43]. There are totally 100 classes and 600 examples in each class. For evaluation, we follow the split of [39] and use 64 of 100 classes for meta-training, 16 for validation, and 20 for meta-test (model evaluation). In other words, a model is trained on few-shot tasks sampled from the 64 SEEN classes set during meta-training, and the best model is selected based on the few-shot classification performance over the 16 class set. The final model is evaluated based on few-shot tasks sampled from the 20 UNSEEN classes.

The *TieredImageNet* [42] is a more complicated version compared with the *MiniImageNet*. It contains 34 super-categories in total, with 20 for meta-training, 6 for validation (meta-val), and 8 for model testing (meta-test). Each of the super-category has 10 to 30 classes. In detail, there are 351, 97, and 160 classes for meta-training, meta-validation, and meta-test, respectively. The divergence of the super-concept leads to a more difficult few-shot classification problem.

Since both datasets are constructed by images from ILSVRC-12, we augment the *meta-training* set of each dataset by sampling non-overlapping images from the corresponding classes in ILSVRC-12. The auxiliary meta-train set is used to measure the generalized few-shot learning classification performance on the SEEN class set. For example, for each of the 64 SEEN classes in the *MiniImageNet*, we collect 200 more non-overlapping images per class from ILSVRC-12 as the test set for many-shot classification. The illustration of the dataset split is shown in Figure 4.

6.2 Baselines and Prior Methods

We explore several (strong) choices in deriving classifiers for the SEEN and UNSEEN classes:

(1) Multiclass Classifier (MC) + k NN. A $|\mathcal{S}|$ -way classifier is trained on the SEEN classes in a supervised learning manner as standard many-shot classification [18]. During the inference, test examples of \mathcal{S} categories are evaluated based on the $|\mathcal{S}|$ -way classifiers and $|\mathcal{U}|$ categories are evaluated using the support embeddings from $\mathcal{D}_{\text{train}}^{\mathcal{U}}$ with a nearest neighbor classifier. To evaluate the generalized few-shot classification task, we take the union of multi-class classifiers’ confidence and nearest neighbor confidence (the normalized negative distance values as in [47]) as joint classification scores on $\mathcal{S} \cup \mathcal{U}$.

(2) ProtoNet + ProtoNet. We train a few-shot classifier (initialized by the MC classifier’s feature mapping) using the Prototypical Network [47] (a.k.a ProtoNet), pretending they were few-shot. When evaluated on the SEEN categories, we randomly sample 100 training instances per category to compute the class prototypes. The class prototypes of UNSEEN classes are computed based on the sampled few-shot training set. During the inference of *generalized* few-shot learning, the confidence of a test instances is jointly determined by its (negative) distance to both SEEN and UNSEEN class prototypes.

(3) MC + ProtoNet. We combine the learning objective of the previous two baselines ((1) and (2)) to jointly learn the MC classifier and feature embedding. Since there are two objectives for many-shot (cross-entropy loss on all SEEN classes) and few-shot (ProtoNet meta-learning objective) classification respectively, it trades off between many-shot and few-shot learning. Therefore, this learned model can be used as multi-class linear classifiers on the “head” categories, and used as ProtoNet on the “tail” categories. During the inference, the model predicts instances from SEEN class \mathcal{S} with the MC classifier, while takes advantage of the few-shot prototypes to discern UNSEEN class

Table 2: Generalized Few-shot classification performance (mean accuracy, Δ -value, and harmonic mean accuracy) on *MiniImageNet* when there are **64 Head and 5 Tail categories**.

Setups Perf. Measures	1-Shot		5-Shot		1-Shot	5-Shot
	Mean Acc. \uparrow	Δ \downarrow	Mean Acc. \uparrow	Δ \downarrow	Harmonic	Mean Acc. \uparrow
IFSL [41]	54.95 \pm 0.30	11.84	63.04 \pm 0.30	10.66	-	-
L2ML [58]	46.25 \pm 0.04	27.49	45.81 \pm 0.03	35.53	2.98 \pm 0.06	1.12 \pm 0.04
DFSL [15]	61.00 \pm 0.11	13.28	72.84 \pm 0.09	10.58	59.96 \pm 0.13	72.42 \pm 0.09
MC + k NN	46.96 \pm 0.03	27.19	45.50 \pm 0.03	38.45	0.00 \pm 0.00	0.00 \pm 0.00
MC + ProtoNet	45.21 \pm 0.03	30.72	45.52 \pm 0.03	38.94	0.00 \pm 0.00	0.00 \pm 0.00
ProtoNet + ProtoNet	53.93 \pm 0.08	22.09	72.64 \pm 0.08	11.41	27.73 \pm 0.19	68.99 \pm 0.11
Ours: CASTLE	66.48 \pm 0.11	9.94	76.25 \pm 0.09	8.14	64.29 \pm 0.14	75.79 \pm 0.10
Ours: ACASTLE	67.49\pm0.11	9.15	77.09\pm0.09	7.74	65.21\pm0.14	76.56\pm0.10

instances. To evaluate the generalized few-shot classification task, we take the union of multi-class classifiers’ confidence and ProtoNet confidence as joint classification scores on $\mathcal{S} \cup \mathcal{U}$.

(4) **L2ML.** Wang *et al.* [58] propose learning to model the “tail” (L2ML) by connecting a few-shot classifier with the corresponding many-shot classifier. The method is designed to learn classifier dynamics from data-poor “tail” classes to the data-rich “head” classes. Since L2ML is originally designed to learn with both SEEN and UNSEEN classes in a transductive manner. In our experiment, we adaptive it to our setting. Therefore, we learn a classifier mapping based on the sampled few-shot tasks from SEEN class set \mathcal{S} , which transforms a few-shot classifier in UNSEEN class set \mathcal{U} inductively. Following [58], we first train a many-shot classifier W upon the ResNet backbone on the SEEN class set \mathcal{S} . We use the same residual architecture as in [58] to implement the classifier mapping f , which transforms a few-shot classifier to a many-shot classifier. During the meta-learning stage, a \mathcal{S} -way few-shot task is sampled in each mini-batch, which produces a \mathcal{S} -way linear few-shot classifier \hat{W} based on the fixed pre-trained embedding. The objective of L2ML not only regresses the mapped few-shot classifier $f(\hat{W})$ close to the many-shot one W measured by square loss, but also minimizes the classification loss of $f(\hat{W})$ over a randomly sampled instances from \mathcal{S} . Therefore, L2ML uses a pre-trained multi-class classifier W for those “head” categories, and used the predicted few-shot classifiers with f for the “tail” categories.

Besides, we also compare our approach with the Dynamic Few-Shot Learning without forgetting (DFSL) [15] and the newly proposed Incremental few-shot learning (IFSL) [41]. For CASTLE, we use the many-shot classifiers $\{\Theta_{\mathcal{S}}\}$, cf. Section 3.1) for the SEEN classes and the synthesized classifiers for the UNSEEN classes to classify an instance into all classes, and then select the prediction with the highest confidence score. For ACASTLE, we adapt the “head” classifiers to $\{\hat{\Theta}_{\mathcal{S}}\}$ with the help of the “tail” classes.

6.3 Main Results

We first test all GFSL methods on *MiniImageNet* with the criteria in [15, 41], the mean accuracy over all classes (the higher the better) and the Δ -value (the lower the better). An effective GFSL approach not only makes prediction well on the joint label space (with high accuracy) but also keeps its classification ability when changing from many-shot/few-shot to the generalized few-shot case (low Δ -value).

The main results are shown in Table 2. We found that ACASTLE outperforms all the existing methods as well as our proposed baseline systems in terms of the mean accuracy. Meanwhile, when looked at the Δ -value, and CASTLE variants are the least affected between predicting for SEEN/UNSEEN classes separately and predicting over all classes jointly.

However, we find that either mean accuracy or Δ -value is not informative enough to tell about a GFSL algorithm’s performances. For example, a baseline system, *i.e.* ProtoNet + ProtoNet performs better than IFSL in terms of 5-shot mean accuracy but not Δ -value. This is consistent with the observation in [41] that the Δ -value should be considered together with the mean accuracy. *In this case, how shall we rank these two systems?* To answer this question, we propose to use another evaluation

Table 3: Generalized Few-shot classification accuracies on *MiniImageNet* with **64 head categories and 20 tail categories**.

Classification on Perf. Measures	20 UNSEEN Categories $\mathcal{U} \rightarrow \mathcal{U}$		64 SEEN + 20 UNSEEN Categories					
			$\mathcal{S} \rightarrow \mathcal{S} \cup \mathcal{U}$		$\mathcal{U} \rightarrow \mathcal{S} \cup \mathcal{U}$		<i>HM Acc.</i>	
Setups	1-Shot	5-Shot	1-Shot	5-Shot	1-Shot	5-Shot	1-Shot	5-Shot
L2ML [58]	27.79±0.73	43.42±0.63	90.99±0.03	90.99±0.03	0.64±0.00	1.21±0.01	1.27±0.09	2.38±0.02
DFSL [15]	30.03±0.75	49.10±0.63	55.33±0.06	72.91±0.05	29.02±0.07	44.85±0.06	38.07±0.06	55.54±0.05
MC + k NN	27.91±0.73	50.98±0.64	90.98±0.03	90.98±0.03	0.00±0.00	0.00±0.00	0.00±0.00	0.00±0.00
MC + ProtoNet	30.89±0.62	51.76±0.62	90.39±0.03	90.99±0.03	0.00±0.00	0.00±0.00	0.00±0.00	0.00±0.00
ProtoNet + ProtoNet	30.54±0.77	51.64±0.62	87.35±0.04	85.08±0.04	14.46±0.05	41.22±0.06	24.81±0.08	55.90±0.06
Ours: CASTLE	33.42±0.75	52.95±0.62	61.46±0.06	73.64±0.06	30.46±0.08	47.55±0.05	40.73±0.07	57.78±0.07
Ours: ACASTLE	33.62±0.75	52.99±0.62	62.46±0.06	76.62±0.06	30.43±0.08	47.58±0.06	40.93±0.07	58.71±0.07

Table 4: Generalized Few-shot classification accuracy on *TieredImageNet* with **351 head categories and 160 tail categories**.

Classification on Perf. Measures	160 UNSEEN Categories $\mathcal{U} \rightarrow \mathcal{U}$		351 SEEN + 160 UNSEEN Categories					
			$\mathcal{S} \rightarrow \mathcal{S} \cup \mathcal{U}$		$\mathcal{U} \rightarrow \mathcal{S} \cup \mathcal{U}$		<i>HM Acc.</i>	
Setups	1-Shot	5-Shot	1-Shot	5-Shot	1-Shot	5-Shot	1-Shot	5-Shot
DFSL [15]	14.56±0.42	28.35±0.40	11.29±0.05	14.95±0.06	14.24±0.06	27.22±0.07	12.60±0.11	19.29±0.05
MC + k NN	12.37±0.41	25.70±0.40	63.96±0.07	63.91±0.07	0.00±0.00	0.00±0.00	0.01±0.00	0.01±0.00
MC + ProtoNet	12.84±0.41	26.89±0.42	63.97±0.07	63.92±0.07	0.00±0.00	0.00±0.00	0.00±0.00	0.00±0.00
ProtoNet + ProtoNet	12.98±0.42	27.00±0.41	54.57±0.08	56.82±0.07	3.65±0.03	19.16±0.06	6.84±0.05	28.66±0.07
Ours: CASTLE	14.86±0.20	28.55±0.41	22.82±0.08	25.88±0.08	14.72±0.06	35.62±0.05	17.89±0.51	29.96±0.05
Ours: ACASTLE	14.91±0.20	28.62±0.41	23.83±0.08	26.12±0.08	14.71±0.06	35.20±0.05	18.19±0.51	29.97±0.05

measure, the harmonic mean of the mean accuracy for each SEEN and UNSEEN category [45, 59], when they are classified jointly.

Harmonic mean accuracy measures GFSL performance better. Since the number of SEEN and UNSEEN classes are most likely to be not equal, *e.g.*, 64 vs. 5 in our cases, directly computing the mean accuracy over all classes is almost always biased. For example, a many-shot classifier that only classifies samples into SEEN classes can receive a good performance than one that recognizes both SEEN and UNSEEN. Therefore, we argue that *harmonic mean* over the mean accuracy can better assess a classifier’s performance, as now the performances are negatively affected when a classifier ignores classes (*e.g.*, MC classifier get 0% harmonic mean). Specifically, we compute the top-1 accuracy for instances from SEEN and UNSEEN classes, and take their harmonic mean as the performance measure. The results are included in the right side of the Table 2.

We find the harmonic mean accuracy takes a holistic consideration of the “absolute” joint classification performance and the “relative” performance drop when classifying towards the joint set. For example, the many-shot baseline MC+ k NN with good mean accuracy and high Δ -value has extremely low performance as it tends to ignore UNSEEN categories. Meanwhile, CASTLE and ACASTLE remains the best when ranked by the harmonic mean accuracy against others.

Evaluate GFSL beyond 5 UNSEEN categories. Besides using harmonic mean accuracy, we argue that another important aspect in evaluating GFSL is to go beyond the 5 sampled UNSEEN categories, as it is never the case in real-world. On the contrary, we care most about the GFSL with a large number of UNSEEN classes. To this end, we consider an extreme case – evaluating GFSL with *all available* SEEN and UNSEEN categories over both *MiniImageNet* and *TieredImageNet*, and report their results in Table 3 and Table 4.

Together with the harmonic mean accuracy of *all* categories, we also report the “tail” classification performance, which is a more challenging few-shot classification task (the standard FSL results could be found in Section 6.5). In addition, the joint classification accuracy for SEEN classes instances ($\mathcal{S} \rightarrow \mathcal{S} \cup \mathcal{U}$) and UNSEEN classes instances ($\mathcal{U} \rightarrow \mathcal{S} \cup \mathcal{U}$) are also listed.

The methods without a clear consideration of “head”-“tail” trade-off (*e.g.*, ProtoNet+ProtoNet) fails to make a joint prediction over both SEEN and UNSEEN classes. We observe that CASTLE and ACASTLE

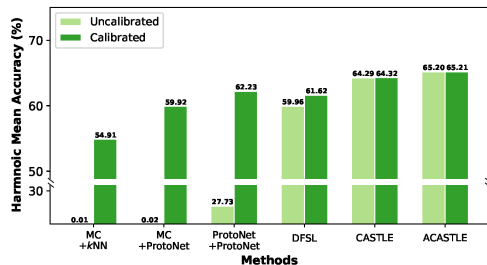


Figure 7: Calibration’s effect to the 1-shot harmonic mean accuracy on *MiniImageNet*. Baseline models improve a lot with the help of the calibration factor.

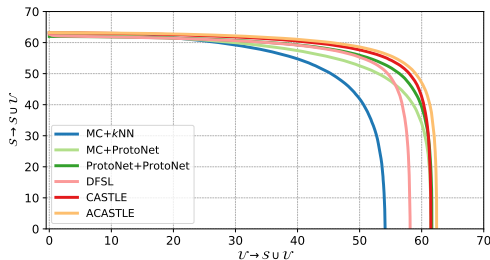


Figure 8: The 1-shot AUSUC performance with two configurations of UNSEEN classes on *MiniImageNet*. The larger the area under the curve, the better the GFSL ability.

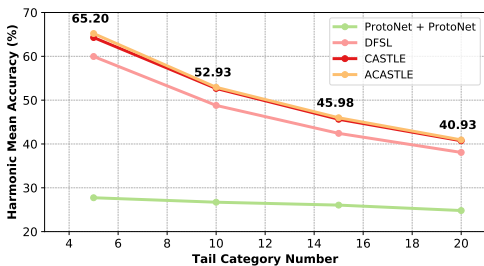


Figure 9: Results of 1-shot GFSL harmonic mean accuracy with incremental number of UNSEEN classes on *MiniImageNet*. Note MC+kNN and MC+ProtoNet bias towards SEEN classes and get nearly zero harmonic mean accuracy.

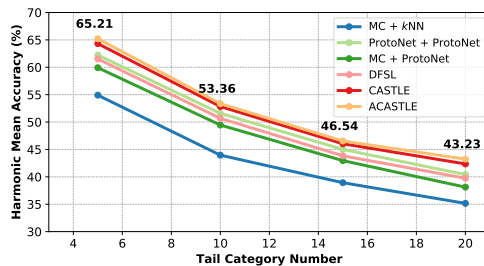


Figure 10: Post-calibrated results of 1-shot GFSL harmonic mean accuracy with incremental number of UNSEEN classes on *MiniImageNet*. All methods select their best calibration factors from the meta-validation data split.

outperform all approaches in the UNSEEN and more importantly, the ALL categories section, across two datasets.

Confidence calibration matters in GFSL. In generalized zero-shot learning, [9] has identified a significant prediction bias between classification confidence of SEEN and UNSEEN classifiers. We find a similar phenomena in GFSL. For instance, *ProtoNet + ProtoNet* baseline has a very confident classifier on SEEN categories than UNSEEN categories (The scale of confidence is on average 2.1 times higher). To address this issue, we compute a calibration factor based on the meta-validation set of UNSEEN categories, such that the prediction logits are calibrated by subtracting this factor out from the confidence of SEEN categories’ predictions. With 5 UNSEEN classes from *MiniImageNet*, the GFSL results of all comparison methods before and after calibration is shown in Figure 7. We observe a consistent and obvious improvements over the harmonic mean accuracy for all methods. For example, the FSL method *ProtoNet* gets even better harmonic mean accuracy compared with DFSL (62.33% vs. 61.62%) with such post-calibration, which *becomes a very strong GFSL baseline*. Note that CASTLE and ACASTLE are the least affected with the selected calibration factor. This suggests that CASTLE variants, learned with the unified GFSL objective, have a well-calibrated classification confidence and does not require additional data and extra learning phase to search this calibration factor.

Moreover, we use area under SEEN-UNSEEN curve (AUSUC) as a measure of different GFSL algorithms [9]. Here, AUSUC is a performance measure that takes the effects of the calibration factor out. To do so, we enumerate through a large range of calibration factors and subtract it from the confidence score of SEEN classifiers. Through this process, the joint prediction performances over SEEN and UNSEEN categories, denoted as $S \rightarrow S \cup U$ and $U \rightarrow S \cup U$, shall vary as the calibration factor changes. For instance, when the calibration factor is infinitely large, we measure a classifier that only predicts UNSEEN categories. We denote this as the SEEN-UNSEEN curve. The 1-shot GFSL results with 5 UNSEEN classes from *MiniImageNet* is shown in Figure 8. As a result, we observe that ACASTLE and CASTLE archive the largest area under the curve, which indicates that CASTLE variants are in general a better algorithm over others among different calibration factors.

Table 5: The difference between training with a pre-trained backbone or from scratch with 1-Shot 5-Way Tasks on *MiniImageNet*. “MA” and “HM” denote the *Mean Accuracy* and *Harmonic Mean Accuracy*, respectively.

Perf. Measures	FSL MA	GFSL HM
CASTLE w/ pre-train	63.06 ± 0.21	64.29 ± 0.14
CASTLE w/o pre-train	63.76 ± 0.21	36.64 ± 0.09

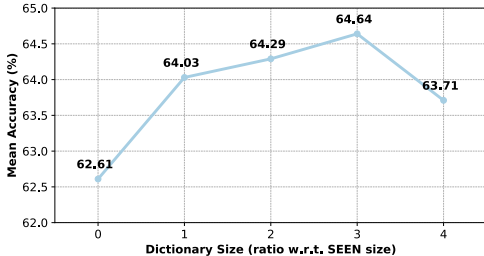


Figure 11: The 1-shot 5-way accuracy on UNSEEN of *MiniImageNet* with different size of dictionaries.

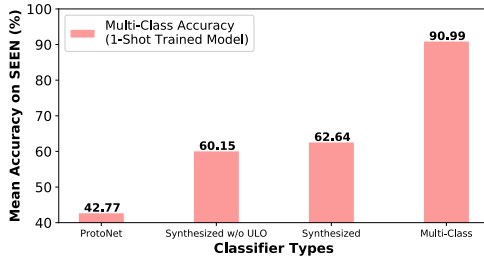


Figure 12: The 64-way multi-class accuracy on SEEN of *MiniImageNet* with 1-shot trained model.

Robust evaluation of GFSL. Other than the harmonic mean accuracy of all SEEN and UNSEEN categories shown in cf. Table 3 and 4, we study the dynamic of how harmonic mean accuracy changes with an incremental number of UNSEEN “tail” concepts. In other words, we show the GFSL performances w.r.t. different numbers of “tail” concepts. We use this as a *robust evaluation* of each system’s GFSL capability. In addition to the test instances from the “head” 64 classes in *MiniImageNet*, 5 to 20 novel classes are included to compose the generalized few-shot tasks. Concretely, only one instance per novel class are used to construct the “tail” classifier, combined with which the model is asked to do a *joint* classification of both SEEN and UNSEEN classes. Figure 9 records the change of generalized few-shot learning performance (harmonic mean) when more UNSEEN classes emerge. We omit the results of MC+kNN and MC+ProtoNet since they bias towards SEEN classes and get nearly zero harmonic mean accuracy in all cases. We observe that ACASTLE consistently outperforms all baseline approaches in each evaluation setup, with a clear margin. We also compute the harmonic mean after selecting the best calibration factor from the meta-val set (cf. Figure 10). It is obvious that almost all baseline models achieve improvements and the phenomenon is consistent with Figure 7. The GFSL results of ACASTLE and CASTLE are almost not influenced after using the post-calibration technique. ACASTLE still persists its superiority in this case.

6.4 Analysis

In this section, we do analyses to show the influence of training a GFSL model by reusing the many-shot classifier and study different implementation choices in the proposed methods. We investigate and provide the results over CASTLE on *MiniImageNet*. We observe the results on ACASTLE reveal similar trends.

Reusing the many-shot classifier facilitates the calibration for GFSL. We compare the strategy to train CASTLE from scratch and fine-tune based on the many-shot classifier. We show both the results of 1-Shot 5-Way few-shot classification performance and GFSL performance with 5 UNSEEN tasks for CASTLE when trained from random or with provided initialization. From the results in Table 5, we find training from scratch gets similar few-shot classification results with the fine-tune strategy, but lower GFSL harmonic mean accuracy. Therefore, reusing the parameters in the many-shot classifier benefits the predictions on SEEN and UNSEEN classes of a GFSL model. Therefore, we use the pre-trained embedding to initialize the backbone.

Effects on the neural dictionary size $|\mathcal{B}|$. We show the effects of the dictionary size (as the ratio of SEEN class size 64) for the generalized few-shot learning (measured by harmonic mean accuracy when there are 5 UNSEEN classes) in Figure 11. We observe that the neural dictionary with a ratio of 2 or 3 works best amongst all other dictionary sizes. Therefore, we fix the dictionary size as 128 across all experiments. Note that when $|\mathcal{B}| = 0$, our method degenerates to case optimizing the unified objective in Eq. 3 without using the neural dictionary (the CASTLE⁻ model in Section 5).

Table 6: The performance with different choices of classifier synthesize strategies when tested with 5-Shot 5-Way UNSEN Tasks on *MiniImageNet*. We denote the option compute embedding prototype and average synthesized classifiers as “Pre-AVG” and “Post-AVG” respectively.

Perf. Measures	FSL <i>Mean Acc.</i>	GFSL <i>HM Acc.</i>
CASTLE w/ Pre-AVG	79.34 ± 0.01	75.59 ± 0.10
CASTLE w/ Post-AVG	79.36 ± 0.01	75.32 ± 0.09

Table 7: The performance change with different number of classifiers (# of CLS) when tested with 1-Shot 5-Way UNSEN Tasks on *MiniImageNet*.

# of Classifiers	1	64	128	256
CASTLE	62.81 ± 0.14	64.02 ± 0.14	64.29 ± 0.14	64.88 ± 0.14

How well is synthesized classifiers comparing with multi-class classifiers? To assess the quality of synthesized classifier, we made a comparison against ProtoNet and also the Multi-class Classifier on the “head” SEEN concepts. To do so, we sample few-shot training instances on each SEEN category to synthesize classifiers (or compute class prototypes for ProtoNet), and then use the synthesized classifiers/class prototypes solely to evaluate multi-class accuracy. The results are shown in Figure 12. We observe that the learned synthesized classifier outperforms over ProtoNet by a large margin. Also, the model trained with unified learning objective improves over the vanilla synthesized classifiers. Note that there is still a significant gap left against multi-class classifiers trained on the entire data set. It suggests that the classifier synthesis we learned is effective against using sole instance embeddings while still far from the many-shot multi-class classifiers.

Different choices of the classifier synthesis. As in Eq. 4, when there is more than one instance per class in a few-shot task (*i.e.*, $K > 1$), CASTLE compute the averaged embeddings first, and then use the prototype of each class as the input of the neural dictionary to synthesize their corresponding classifiers. Here we explore another choice to deal with multiple instances in each class. We synthesize classifiers based on each instance first, and then average the corresponding synthesized classifiers for each class. This option equals an ensemble strategy to average the prediction results of each instance’s synthesized classifier. We denote the pre-average strategy (the one used in CASTLE) as “Pre-AVG”, and the post-average strategy as “Post-AVG”. The 5-Shot 5-way classification results on *MiniImageNet* for these two strategies are shown in Table 6. From the results, “Post-AVG” does not improve the FSL and GFSL performance obviously. Since averaging the synthesized classifiers in a hindsight way costs more memory during meta-training, we choose the “Pre-AVG” option to synthesize classifiers when there are more than 1 shot in each class. In our experiments, the same conclusion also applies to ACASTLE.

How is multiple classifiers learning’s impact over the training? Both CASTLE and ACASTLE adopts a multi-classifier training strategy (cf. Section 3), *i.e.* considering multiple GFSL tasks with different combinations of classifiers in a single mini-batch. In Table 7, we show the influence of the multi-classifier training method based on their FSL and GFSL performance. It shows that with a large number of classifiers during the training, the performance of CASTLE asymptotically converges to its upper-bound. Note that ACASTLE shares a similar trend.

6.5 Standard Few-Shot Learning

Finally, we also evaluate our proposed approaches’ performance on two standard few-shot learning benchmarks, *i.e.*, *MiniImageNet* and *TieredImageNet* data set. We compare our approaches with the state-of-the-art methods in both 1-shot 5-way and 5-shot 5-way scenarios. We cite the results of the comparison methods from their published papers and remark the backbones used to train the FSL model by different methods. The mean accuracy and 95% confidence interval are shown in the Table 8 and Table 9.

It is notable that some comparison methods such as CTM [29] are evaluated over only 600 UNSEN class FSL tasks, while we test both CASTLE and ACASTLE over 10,000 tasks, leading to more stable results. CASTLE and ACASTLE achieve the best 1-shot classification results on both data sets,

Table 8: Few-shot classification accuracy on *MiniImageNet* with different types of backbones. Our methods are evaluated with 10,000 few-shot tasks.

Setups	Backbone	1-Shot 5-Way	5-Shot 5-Way
IFSL [41]	ResNet-10	55.72 ± 0.41	70.50 ± 0.36
DFSL [15]	ResNet-10	56.20 ± 0.86	73.00 ± 0.64
ProtoNet [47]	ResNet-12	61.40 ± 0.12	76.56 ± 0.20
TapNet [61]	ResNet-12	61.65 ± 0.15	76.36 ± 0.10
MetaOptNet [26]	ResNet-12	62.64 ± 0.61	78.63 ± 0.46
FEAT [60]	ResNet-12	62.96 ± 0.20	78.49 ± 0.12
SimpleShot [56]	ResNet-18	62.85 ± 0.20	80.02 ± 0.14
CTM [29]	ResNet-18	64.12 ± 0.82	80.51 ± 0.13
LEO [44]	WRN	61.76 ± 0.08	77.59 ± 0.12
Ours: CASTLE	ResNet-12	63.06 ± 0.21	79.33 ± 0.12
Ours: ACASTLE	ResNet-12	64.17 ± 0.21	79.53 ± 0.12

Table 9: Few-shot classification accuracy on *TieredImageNet* with different types of backbones. Our methods are evaluated with 10,000 few-shot tasks.

Setups	Backbone	1-Shot 5-Way	5-Shot 5-Way
ProtoNet [47]	ConvNet	53.31 ± 0.89	72.69 ± 0.74
RelationNet [48]	ConvNet	54.48 ± 0.93	71.32 ± 0.78
IFSL [41]	ResNet-18	51.12 ± 0.45	66.40 ± 0.36
DFSL [15]	ResNet-18	50.90 ± 0.46	66.69 ± 0.36
TapNet [61]	ResNet-12	63.08 ± 0.15	80.26 ± 0.12
MetaOptNet [26]	ResNet-12	65.99 ± 0.72	81.56 ± 0.63
SimpleShot [56]	ResNet-18	69.09 ± 0.22	84.58 ± 0.16
CTM [29]	ResNet-18	68.41 ± 0.39	84.28 ± 1.73
LEO [44]	WRN	66.33 ± 0.05	81.44 ± 0.09
Ours: CASTLE	ResNet-12	69.06 ± 0.02	83.99 ± 0.16
Ours: ACASTLE	ResNet-12	69.53 ± 0.02	83.83 ± 0.16

and competitive 5-shot classification results with a bit weaker backbone (ResNet-12 compared with ResNet-18 used in other methods). The results support our hypothesis that jointly learning with many-shot classification forces few-shot classifiers to be discriminative.

7 Related Work and Discussion

Building a high-quality visual system usually requires to have a large scale of annotated training set with many shots per category. Many large-scale data sets such as ImageNet have an ample number of instances for popular classes [23, 43]. However, the data-scarce “tail” of the category distribution matters. For example, a visual search engine needs to deal with the rare object of interests (*e.g.*, endangered species) or newly defined items (*e.g.*, new smartphone models), which only possesses a few data instances. Directly training a system over all classes is prone to over-fit and can be biased towards the data-rich categories [5, 11].

Zero-shot learning (ZSL) [2, 7, 24, 59] is a popular idea for addressing learning without labeled data. By aligning the visual and semantic definitions of objects, ZSL transfers the relationship between images and attributes learned from SEEN classes to UNSEEN ones, so as to recognize a novel instance with only its category-wise attributes [6, 8]. Generalized ZSL [9, 45] extends this by calibrating a prediction bias to jointly predict between SEEN and UNSEEN classes. ZSL is limited to recognizing objects with well-defined semantic descriptions, which assumes that the visual appearance of novel categories is harder to obtain than knowledge about their attributes, whereas in the real-world we often get the appearance of objects before learning about their characteristics.

Few-shot learning (FSL) proposes a more realistic setup, where we have access to a very limited number (instead of zero) of visual exemplars from the “tail” classes [28, 52]. FSL meta-learns an inductive bias from the SEEN classes, such that it transfers to the learning process of UNSEEN classes with few training data during the model deployment. For example, one line of works uses meta-learned discriminative feature embeddings [1, 26, 36, 44, 47, 60] together with the non-parametric nearest neighbor classifiers, to recognize novel classes given a few exemplars. Another line of works chooses to learn the common optimization strategy [4, 39] across few-shot tasks, *e.g.*, the model initialization to a pre-specified model configuration could be adapted rapidly using fixed steps of gradient descents over the few-shot training data from UNSEEN categories [3, 13, 27, 30, 35, 53]. FSL has achieved promising results in various domains such as visual recognition [31, 49], domain adaptation [12, 19], neural machine translation [16], data compression [55], and density estimation [40]. Empirical studies of FSL could be found in [10, 50].

FSL emphasizes on building models of the UNSEEN classes and *ignores its real-world use case of assisting the many-shot recognition of the “head” categories*. A more realistic setting, *i.e.*, low-shot learning, has been studied before [14, 17, 32, 57, 60]. The main aim is to recognize the entire set of concepts in a transductive learning framework — during the training of the target model, you have access to both the (many-shot) SEEN and (few-shot) UNSEEN categories. The key difference with our Generalized Few-Shot Learning (GFSL) is that we assume no access to UNSEEN classes in the model

learning phase, which requires the model to *inductively* transfer knowledge from SEEN classes to UNSEEN ones during the model evaluation phase.

Some of the previous GFSL approaches [14, 17, 57] apply the exemplar-based classification paradigms on both SEEN and UNSEEN categories to resolve the transductive learning problem, which requires recomputing the centroids for SEEN categories after model updates. Others [32, 45, 58] usually ignore the explicit relationship between SEEN and UNSEEN categories, and learn separate classifiers. [15, 41] propose to solve inductive GFSL via either composing UNSEEN with SEEN classifiers or meta-learning with recurrent back-propagation procedure. Gidaris *et al* [15] is the most related work to CASTLE and ACASTLE, which composes the “tail” classifiers by a convex combination of the many-shot classifiers. CASTLE is different from Gidaris *et al* [15] as it presents an *end-to-end learnable framework* with improved training techniques, as well as it employs a *shared neural dictionary* to compose few-shot classifiers. Moreover, ACASTLE further relates the knowledge for both SEEN and UNSEEN classes by constructing a neural dictionary with both shared (yet task-agnostic) and task-specific basis, which allows backward knowledge transfer to benefit SEEN classifiers with new knowledge of UNSEEN classes. As we have demonstrated in Section 5, ACASTLE significantly improves SEEN classifiers when learning of UNSEEN visual categories over heterogeneous visual domains.

8 Conclusion

A Generalized Few-Shot Learning (GFSL) model takes both the discriminative ability of many-shot and few-shot classifiers into account. In this paper, we propose the Classifier Synthesis Learning (CASTLE) and its adaptive variant (ACASTLE) to solve the challenging inductive modeling of UNSEEN categories in conjunction with seen ones. Our approach takes advantage of the neural dictionary to learn bases for composing many-shot and few-shot classifiers via a unified learning objective, which can better transfer the knowledge from SEEN to UNSEEN classifiers. Our experiments highlight ACASTLE especially fits the GFSL scenario with tasks from multiple domains. Both CASTLE and ACASTLE not only outperform existing methods in terms of various GFSL criteria but also improve the classifier’s discernibility over standard FSL. Future directions include designing the SEEN class token and neural bases, which would facilitate the task optimization so that the “head” and “tail” classifiers could be fine-tuned based on the current generalized few-shot task.

Acknowledgements

This research is partially supported by the National Key R&D Program of China (2018YFB1004300), NSFC (61773198, 61751306, 61632004), NSF Awards IIS-1513966/ 1632803/1833137, CCF-1139148, DARPA Award#: FA8750-18-2-0117, DARPA-D3M - Award UCB-00009528, Google Research Awards, gifts from Facebook and Netflix, and ARO# W911NF-12-1-0241 and W911NF-15-1-0484.

References

- [1] Multimodal model-agnostic meta-learning via task-aware modulation. In: Advances in Neural Information Processing Systems 32, pp. 1–12. Curran Associates, Inc. (2019) 19
- [2] Akata, Z., Perronnin, F., Harchaoui, Z., Schmid, C.: Label-embedding for attribute-based classification. In: IEEE Conference on Computer Vision and Pattern Recognition, pp. 819–826. Portland, OR (2013) 19
- [3] Antoniou, A., Edwards, H., Storkey, A.J.: How to train your MAML. In: Proceedings of the 3rd International Conference on Learning Representations. New Orleans, LA (2019) 2, 19
- [4] Bertinetto, L., Henriques, J.F., Torr, P.H.S., Vedaldi, A.: Meta-learning with differentiable closed-form solvers. In: Proceedings of the 7th International Conference on Learning Representations. New Orleans, LA (2019) 8, 19
- [5] Cao, K., Wei, C., Gaidon, A., Arechiga, N., Ma, T.: Learning imbalanced datasets with label-distribution-aware margin loss. In: Advances in Neural Information Processing Systems 32, pp. 1565–1576. Curran Associates, Inc. (2019) 2, 19

- [6] Changpinyo, S., Chao, W.L., Gong, B., Sha, F.: Synthesized classifiers for zero-shot learning. In: IEEE Conference on Computer Vision and Pattern Recognition, pp. 5327–5336. Las Vegas, NV (2016) [7](#), [19](#)
- [7] Changpinyo, S., Chao, W.L., Gong, B., Sha, F.: Classifier and exemplar synthesis for zero-shot learning. CoRR [abs/1812.06423](#) (2018) [7](#), [19](#)
- [8] Changpinyo, S., Chao, W.L., Sha, F.: Predicting visual exemplars of unseen classes for zero-shot learning. In: 2017 IEEE International Conference on Computer Vision (ICCV), pp. 3496–3505. Venice, Italy (2017) [19](#)
- [9] Chao, W.L., Changpinyo, S., Gong, B., Sha, F.: An empirical study and analysis of generalized zero-shot learning for object recognition in the wild. In: Proceedings of the 14th European Conference on Computer Vision, pp. 52–68. Amsterdam, The Netherlands (2016) [2](#), [10](#), [16](#), [19](#)
- [10] Chen, W.Y., Liu, Y.C., Kira, Z., Wang, Y.C.F., Huang, J.B.: A closer look at few-shot classification. In: Proceedings of the 3rd International Conference on Learning Representations. New Orleans, LA (2019) [19](#)
- [11] Cui, Y., Jia, M., Lin, T.Y., Song, Y., Belongie, S.J.: Class-balanced loss based on effective number of samples. In: IEEE Conference on Computer Vision and Pattern Recognition, pp. 9268–9277. Long Beach, CA (2019) [2](#), [19](#)
- [12] Dong, N., Xing, E.P.: Domain adaption in one-shot learning. In: Proceedings of the European Conference on Machine Learning and Knowledge Discovery in Databases, pp. 573–588. Dublin, Ireland (2018) [19](#)
- [13] Finn, C., Abbeel, P., Levine, S.: Model-agnostic meta-learning for fast adaptation of deep networks. In: Proceedings of the 34th International Conference on Machine Learning, pp. 1126–1135. Sydney, Australia (2017) [1](#), [2](#), [4](#), [9](#), [19](#)
- [14] Gao, H., Shou, Z., Zareian, A., Zhang, H., Chang, S.F.: Low-shot learning via covariance-preserving adversarial augmentation networks. In: Advances in Neural Information Processing Systems 31, pp. 983–993. Curran Associates, Inc. (2018) [19](#), [20](#)
- [15] Gidaris, S., Komodakis, N.: Dynamic few-shot visual learning without forgetting. In: IEEE International Conference on Computer Vision, pp. 4367–4375. Salt Lake City, UT (2018) [7](#), [8](#), [9](#), [11](#), [12](#), [14](#), [15](#), [19](#), [20](#)
- [16] Gu, J., Wang, Y., Chen, Y., Li, V.O.K., Cho, K.: Meta-learning for low-resource neural machine translation. In: Proceedings of the 2018 Conference on Empirical Methods in Natural Language Processing, pp. 3622–3631. Brussels, Belgium (2018) [19](#)
- [17] Hariharan, B., Girshick, R.B.: Low-shot visual recognition by shrinking and hallucinating features. In: IEEE International Conference on Computer Vision, pp. 3037–3046. Venice, Italy (2017) [2](#), [19](#), [20](#)
- [18] He, K., Zhang, X., Ren, S., Sun, J.: Deep residual learning for image recognition. In: IEEE Conference on Computer Vision and Pattern Recognition, pp. 770–778. Las Vegas, NV (2016) [1](#), [8](#), [13](#)
- [19] Kang, B., Feng, J.: Transferable meta learning across domains. In: Proceedings of the 34th Conference on Uncertainty in Artificial Intelligence, pp. 177–187. Monteret, CA (2018) [19](#)
- [20] Khosla, A., Jayadevaprakash, N., Yao, B., Fei-Fei, L.: Novel dataset for fine-grained image categorization. In: 1st Workshop on Fine-Grained Visual Categorization, IEEE Conference on Computer Vision and Pattern Recognition. Colorado Springs, CO (2011) [11](#)
- [21] Koch, G., Zemel, R., Salakhutdinov, R.: Siamese neural networks for one-shot image recognition. In: ICML Deep Learning Workshop, vol. 2 (2015) [4](#)
- [22] Krause, J., Stark, M., Deng, J., Fei-Fei, L.: 3d object representations for fine-grained categorization. In: 4th International IEEE Workshop on 3D Representation and Recognition (3dRR-13). Sydney, Australia (2013) [11](#)
- [23] Krizhevsky, A., Sutskever, I., Hinton, G.E.: Imagenet classification with deep convolutional neural networks. Communications of the ACM [60](#)(6), 84–90 (2017) [1](#), [19](#)
- [24] Lampert, C.H., Nickisch, H., Harmeling, S.: Attribute-based classification for zero-shot visual object categorization. IEEE Transactions on Pattern Analysis and Machine Intelligence [36](#)(3), 453–465 (2014) [19](#)

- [25] Larochelle, H.: Few-shot learning with meta-learning: Progress made and challenges ahead (2018) [2](#)
- [26] Lee, K., Maji, S., Ravichandran, A., Soatto, S.: Meta-learning with differentiable convex optimization. In: IEEE Conference on Computer Vision and Pattern Recognition, pp. 10657–10665. Long Beach, CA (2019) [2](#), [19](#)
- [27] Lee, Y., Choi, S.: Gradient-based meta-learning with learned layerwise metric and subspace. In: Proceedings of the 35th International Conference on Machine Learning, pp. 2933–2942. Stockholm, Sweden (2018) [19](#)
- [28] Li, F.F., Fergus, R., Perona, P.: One-shot learning of object categories. IEEE Transactions on Pattern Analysis and Machine Intelligence **28**(4), 594–611 (2006) [19](#)
- [29] Li, H., Eigen, D., Dodge, S., Zeiler, M., Wang, X.: Finding task-relevant features for few-shot learning by category traversal. In: IEEE Conference on Computer Vision and Pattern Recognition, pp. 1–10. Long Beach, CA (2019) [18](#), [19](#)
- [30] Li, Z., Zhou, F., Chen, F., Li, H.: Meta-sgd: Learning to learn quickly for few shot learning. CoRR [abs/1707.09835](#) (2017) [19](#)
- [31] Lifchitz, Y., Avrithis, Y., Picard, S., Bursuc, A.: Dense classification and implanting for few-shot learning. In: IEEE Conference on Computer Vision and Pattern Recognition, pp. 9258–9267. Long Beach, CA (2019) [19](#)
- [32] Liu, Z., Miao, Z., Zhan, X., Wang, J., Gong, B., Yu, S.X.: Large-scale long-tailed recognition in an open world. In: IEEE Conference on Computer Vision and Pattern Recognition, pp. 2537–2546. Long Beach, CA (2019) [1](#), [2](#), [19](#), [20](#)
- [33] Lopez-Paz, D., Ranzato, M.: Gradient episodic memory for continual learning. In: Advances in Neural Information Processing Systems, pp. 6467–6476 (2017) [3](#)
- [34] Maji, S., Kannala, J., Rahtu, E., Blaschko, M., Vedaldi, A.: Fine-grained visual classification of aircraft. Tech. rep. (2013) [11](#)
- [35] Nichol, A., Achiam, J., Schulman, J.: On first-order meta-learning algorithms. CoRR [abs/1803.02999](#) (2018) [2](#), [19](#)
- [36] Oreshkin, B.N., López, P.R., Lacoste, A.: TADAM: task dependent adaptive metric for improved few-shot learning. In: Advances in Neural Information Processing Systems 31, pp. 719–729. Curran Associates, Inc. (2018) [19](#)
- [37] Qiao, S., Liu, C., Shen, W., Yuille, A.L.: Few-shot image recognition by predicting parameters from activations. In: IEEE Conference on Computer Vision and Pattern Recognition, pp. 7229–7238. Salt Lake City, UT (2018) [8](#)
- [38] Quattoni, A., Torralba, A.: Recognizing indoor scenes. In: IEEE Conference on Computer Vision and Pattern Recognition, pp. 413–420. Miami, Florida (2009) [11](#)
- [39] Ravi, S., Larochelle, H.: Optimization as a model for few-shot learning. In: Proceedings of the 5th International Conference on Learning Representations. Toulon, France (2017) [2](#), [13](#), [19](#)
- [40] Reed, S.E., Chen, Y., Paine, T., van den Oord, A., Eslami, S.M.A., Rezende, D.J., Vinyals, O., de Freitas, N.: Few-shot autoregressive density estimation: Towards learning to learn distributions. In: Proceedings of the 6th International Conference on Learning Representations. Vancouver, Canada (2018) [19](#)
- [41] Ren, M., Liao, R., Fetaya, E., Zemel, R.: Incremental few-shot learning with attention attractor networks. In: Advances in Neural Information Processing Systems, pp. 5276–5286. Curran Associates, Inc. (2019) [10](#), [14](#), [19](#), [20](#)
- [42] Ren, M., Triantafillou, E., Ravi, S., Snell, J., Swersky, K., Tenenbaum, J.B., Larochelle, H., Zemel, R.S.: Meta-learning for semi-supervised few-shot classification. In: Proceedings of the 6th International Conference on Learning Representations. Vancouver, Canada (2018) [13](#)
- [43] Russakovsky, O., Deng, J., Su, H., Krause, J., Satheesh, S., Ma, S., Huang, Z., Karpathy, A., Khosla, A., Bernstein, M.S., Berg, A.C., Li, F.F.: Imagenet large scale visual recognition challenge. International Journal of Computer Vision **115**(3), 211–252 (2015) [13](#), [19](#)
- [44] Rusu, A.A., Rao, D., Sygnowski, J., Vinyals, O., Pascanu, R., Osindero, S., Hadsell, R.: Meta-learning with latent embedding optimization. In: Proceedings of the 7th International Conference on Learning Representations. New Orleans, LA (2019) [2](#), [8](#), [19](#)

- [45] Schönfeld, E., Ebrahimi, S., Sinha, S., Darrell, T., Akata, Z.: Generalized zero- and few-shot learning via aligned variational autoencoders. In: IEEE Conference on Computer Vision and Pattern Recognition, pp. 8247–8255. Long Beach, CA (2019) [12](#), [15](#), [19](#), [20](#)
- [46] Simonyan, K., Zisserman, A.: Very deep convolutional networks for large-scale image recognition. CoRR [abs/1409.1556](#) (2014) [1](#)
- [47] Snell, J., Swersky, K., Zemel, R.S.: Prototypical networks for few-shot learning. In: Advances in Neural Information Processing Systems 30, pp. 4080–4090. Curran Associates, Inc. (2017) [1](#), [2](#), [4](#), [9](#), [13](#), [19](#)
- [48] Sung, F., Yang, Y., Zhang, L., Xiang, T., Torr, P.H.S., Hospedales, T.M.: Learning to compare: Relation network for few-shot learning. In: IEEE Conference on Computer Vision and Pattern Recognition, pp. 1199–1208. Salt Lake City, UT (2018) [19](#)
- [49] Triantafillou, E., Zemel, R.S., Urtasun, R.: Few-shot learning through an information retrieval lens. In: Advances in Neural Information Processing Systems 30, pp. 2252–2262. Curran Associates, Inc. (2017) [19](#)
- [50] Triantafillou, E., Zhu, T., Dumoulin, V., Lamblin, P., Xu, K., Goroshin, R., Gelada, C., Swersky, K., Manzagol, P.A., Larochelle, H.: Meta-dataset: A dataset of datasets for learning to learn from few examples. CoRR [abs/1903.03096](#) (2019) [19](#)
- [51] Venkateswara, H., Eusebio, J., Chakraborty, S., Panchanathan, S.: Deep hashing network for unsupervised domain adaptation. In: 2017 IEEE Conference on Computer Vision and Pattern Recognition, pp. 5385–5394. Honolulu, HI (2017) [11](#)
- [52] Vinyals, O., Blundell, C., Lillicrap, T., Kavukcuoglu, K., Wierstra, D.: Matching networks for one shot learning. In: Advances in Neural Information Processing Systems 29, pp. 3630–3638. Curran Associates, Inc. (2016) [1](#), [2](#), [4](#), [9](#), [13](#), [19](#)
- [53] Vuorio, R., Sun, S.H., Hu, H., Lim, J.J.: Toward multimodal model-agnostic meta-learning. CoRR [abs/1812.07172](#) (2018) [19](#)
- [54] Wah, C., Branson, S., Welinder, P., Perona, P., Belongie, S.: The Caltech-UCSD Birds-200-2011 Dataset. Tech. Rep. CNS-TR-2011-001, California Institute of Technology (2011) [11](#)
- [55] Wang, T., Zhu, J.Y., Torralba, A., Efros, A.A.: Dataset distillation. CoRR [abs/1811.10959](#) (2018) [19](#)
- [56] Wang, Y., Chao, W.L., Weinberger, K.Q., van der Maaten, L.: SimpleShot: Revisiting nearest-neighbor classification for few-shot learning. CoRR [abs/1911.04623](#) (2019) [19](#)
- [57] Wang, Y.X., Girshick, R.B., Hebert, M., Hariharan, B.: Low-shot learning from imaginary data. In: Proceedings of the IEEE Conference on Computer Vision and Pattern Recognition, pp. 7278–7286. Salt Lake City, UT (2018) [2](#), [19](#), [20](#)
- [58] Wang, Y.X., Ramanan, D., Hebert, M.: Learning to model the tail. In: Advances in Neural Information Processing Systems 30, pp. 7032–7042. Curran Associates, Inc. (2017) [1](#), [2](#), [9](#), [14](#), [15](#), [20](#)
- [59] Xian, Y., Schiele, B., Akata, Z.: Zero-shot learning - the good, the bad and the ugly. In: 2017 IEEE Conference on Computer Vision and Pattern Recognition, pp. 3077–3086. Honolulu, HI (2017) [10](#), [12](#), [15](#), [19](#)
- [60] Ye, H.J., Hu, H., Zhan, D.C., Sha, F.: Learning embedding adaptation for few-shot learning. CoRR [abs/1812.03664](#) (2018) [2](#), [8](#), [9](#), [19](#)
- [61] Yoon, S.W., Seo, J., Moon, J.: Tapnet: Neural network augmented with task-adaptive projection for few-shot learning. In: Proceedings of the 36th International Conference on Machine Learning, pp. 7115–7123. Long Beach, CA (2019) [19](#)